

Block shear failure mechanism of axially-loaded groups of screws

Ursula Mahlknecht^{a,*}, Reinhard Brandner^b

^a Competence Center holz.bau forschung gmbh, Inffeldgasse 24/1, 8010 Graz, Austria

^b Institute of Timber Engineering and Wood Technology, Graz University of Technology, Inffeldgasse 24/1, 8010 Graz, Austria



ARTICLE INFO

Keywords:

Self-tapping screws
Axially-loaded groups of screws
Failure mechanisms
Block shear failure
Spring model
Group effect

ABSTRACT

Self-tapping screws are fasteners that are versatily applicable in timber engineering. For the design of such screw connections, preferential axial-loading, all possible failure mechanisms have to be considered. Recently, in compact groups of axially-loaded screws the block shear failure mechanism, which has not been investigated so far, turned out to fail rather brittle at load levels lower than currently allowed. This failure mechanism is defined as failure of (rolling) shear and/or tension perpendicular to grain planes encompassing the group of screws. This failure mechanism was observed in groups given a number of different parameter settings, i.e. thread-fibre angles of 90° and 45°, glulam, structural timber and cross laminated timber and various group designs. This paper focuses on groups of axially-loaded screws in glulam and solid timber of Norway spruce (*Picea abies*) and inserted at a thread-fibre angle of 90°. Varying group sizes, loading and supporting distances and group designs, i.e. various penetration lengths l_{ef} and spacing in and perpendicular to grain, a_1 and a_2 , respectively, are analysed by two different “push-pull”-test setups. To predict the block shear capacity and failure characteristics of such groups of screws and to separate this failure mechanism from other failure mechanisms, a mechanical-based block shear model was established. This parallel acting spring model considers load sharing and redistribution between concerned failure planes and depends on a number of material, geometrical and stress distribution parameters. To ensure a reasonable parameter setting, background and potential influencing parameters on each model parameter are discussed. In validation, the model shows overall good predictions of capacities, failure mechanisms and failure sequence for all test series involved. It turned out that the current regulations, comprising the definition of minimum spacing together with minimum edge and end distances, are not sufficient for controlling this three-dimensional block shear failure. In addition, the consideration of the number of screws in the group as well as the penetration length is required.

1. Introduction

1.1. General comments

In contemporary timber engineering, dowel-type fasteners are differentiated in fasteners primary stressed in shear, e.g. dowels or nails, or axially in tension or compression, e.g. self-tapping screws or glued-in rods. Whereas in the first group the timber is primary stressed in compression, in the second group the timber is primary stressed in shear. Self-tapping screws are optimised for load-bearing purposes axial in tension, as addressed in this study, made of hardened steel and feature high resistance and stiffness but only minor plastic deformability until failure. The versatile possibilities how to apply them can be differentiated in “active applications”, i.e. for connecting structural elements, and in “passive applications”, i.e. for reinforcing structural

elements; see Ringhofer et al. [1] and Ringhofer [2].

Active applications with several screws are realised often with outer steel plates, as exemplarily shown in Fig. 1. Differentiation can be made in (i) joints with steel plates constantly pressed on the timber surface, i.e. joints featuring a restricted deformability of the timber surface as shown in Fig. 1(b), named further as “restricted joints”, and in (ii) joints with steel plates constantly taken-off from the timber surface, see Fig. 1(c), named further as “free joints”.

We further concentrate on “free joints” of primary axially and in tension loaded self-tapping screws, thus possible positive effects on the resistance of restricted joints are excluded.

Recent experimental investigations on groups of axially-loaded screws fulfilling all requirements regulated in European standards, e.g. EN 1995-1-1 [3] (Eurocode 5; EC 5) and/or diverse European Technical Approvals/Assessments (ETAs), in particular the requirements on

* Corresponding author.

E-mail address: u.mahlknecht@tugraz.at (U. Mahlknecht).

URLs: <http://www.holzbauforschung.at> (U. Mahlknecht), <http://www.lignum.at> (R. Brandner).

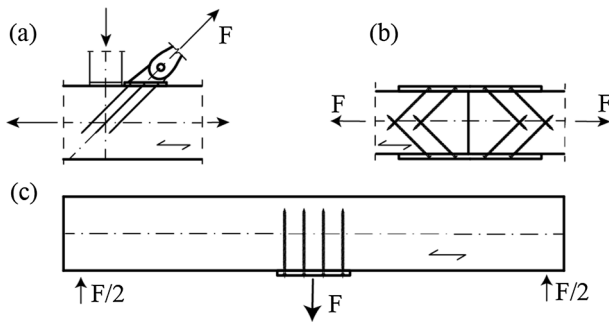


Fig. 1. Examples of joints with groups of screws in active applications: (a) joint in a framework; (b) tensile joint; (c) girder loaded perpendicular to the grain.

spacing and edge and end distances, revealed failure mechanisms with cracks between the rows of screws in grain or at the circumference of the group of screws and/or at their bottom plane. These failure mechanisms could be observed in all so far investigated structural timber products, solid timber (ST), glulam (GLT) and cross laminated timber (CLT), as well as at thread-fibre angles $\alpha = 45^\circ$ and 90° ; see Plieschounig [4], Mahlkecht [5], Mahlkecht and Brandner [6] and Mahlkecht et al. [7] and [8].

Although EC 5 [3] lists block shear as one possible failure mechanism of a group of primary axially-loaded fasteners, design provisions are missing. In fact, apart from references outlined above investigations on this failure mechanism were not reported so far.

The made observations and identified need for design regulations motivate further investigations on this quasi-brittle failure mechanism, which restricts the load-bearing capacity of axially-loaded groups of screws featuring certain geometrical characteristics, i.e. certain combinations of spacing and effective length, as a measure for the anchorage of screws in structural elements.

1.2. Connection design

The design and geometry of joints has to meet structural requirements, should allow an optimal stress distribution and provide an economical solution. The three main principles in structural requirements are high load-bearing capacity, high stiffness and high ductility. Consequently, brittle failure mechanism shall be avoided.

The load-bearing capacity of a joint is limited either by the residual net cross section capacity of the connected structural elements, by the capacity of the fasteners, the capacity of additional joint elements like steel plates or by the capacity of the timber in direct interaction with the group of fasteners.

With a focus on groups of primary axially-loaded self-tapping screws, possible failure mechanisms of single fasteners are: (i) withdrawal, (ii) steel failure in tension or buckling, and (iii) head pull through. Apart from a failure in the net cross section, possible failure mechanisms of the timber surrounding the group of fasteners are: (iv) splitting along the screw rows, and (v) block shear failure mechanisms. The latter failure mechanisms are well known from primary laterally-loaded dowel-type fasteners. In contrast to them, axially-loaded screws introduce the applied load only over the threaded part anchoring the

screw in the penetrated timber member. The main differences between axially- and laterally-loaded groups of dowel-type fasteners are thus the loading direction as well as the type and distribution of stresses. In any case, block and line or row shear failure mechanisms constitute quasi-brittle failure mechanisms of the timber featuring load-bearing capacities below the withdrawal or steel capacity of joints.

According to EC 5 [3], all possible failure mechanisms have to be approved but so far a verification procedure for block shear failure mechanisms of axially-loaded groups of screws is given neither in EC 5 [3] or in ETAs nor in the literature. EC 5 [3] includes constructive rules for the arrangement of screws in a primary axially-loaded group depending on the nominal screw diameter d , e.g. minimum spacing in and perpendicular to the grain, $a_1 = 7d$ and $a_2 = 5d$, respectively, and minimum end and edge distances, $a_{1,CG} = 10d$ and $a_{2,CG} = 4d$, respectively, see Fig. 2(a).

Apart from these geometrical provisions, in determining the leading failure mechanisms further parameters need to be considered: the effective penetration length l_{ef} and the embedment length l_{emb} , see Fig. 2(b). Note: in contrast to EC 5 [3], within this contribution l_{ef} is defined without the length of the screw tip, l_{tip} .

1.3. Group withdrawal and steel failure mechanisms

In case of withdrawal or steel failure mechanism, the capacities of groups of screws can be simply calculated by multiplying the withdrawal capacity, $F_{ax,cs}$, or steel capacity, F_b , of a single screw with the number of fasteners active in resisting the applied load(s), usually given as $n_{ef} \leq n$, with n as the total number of commonly acting fasteners in the group. Whether withdrawal or steel failure occurs depends basically on the effective penetration length, l_{ef} , the material in which the screw is anchored, indicated by the material density ρ , the thread-fibre angle α and the nominal screw diameter d . With respect to steel tension failure, the parameters steel tensile strength and effective net cross section are required.

The effective number of n commonly acting axially-loaded screws in a group on a characteristic (5%-quantile) basis according to EC 5 [3], irrespective of steel or withdrawal failure mechanism, is given as $n_{ef} = n^{0.9}$. Blaß et al. [9] report of tests on double lap tensile joints without a significant influence from the number of screws on joint capacity, indicating $n_{ef} = n$. Plieschounig [4] investigated joints of axially-loaded groups of screws with an outer steel plate as (i) restricted joint and (ii) free joint. In case of (i), joints failed in withdrawal showed $n_{ef} = n$; this was also observed for case (ii), but only for characteristic values (5%-quantiles), whereas for mean values n_{ef}/n decreased significantly with increasing n . Krenn [10] and Krenn and Schickhofer [11] reported on tensile joints realised with screws inclined by 45° and inserted through outer steel plates, designed to screw steel failures. By considering also potential shortcomings in executing such screw joints on-site, for the 5%-quantile values $n_{ef} = 0.9n$ is proposed.

1.4. Block shear and related failure mechanisms

1.4.1. General remarks

Block shear and related failure mechanisms of axially-loaded groups of screws are characterized by tearing-out of a timber volume in

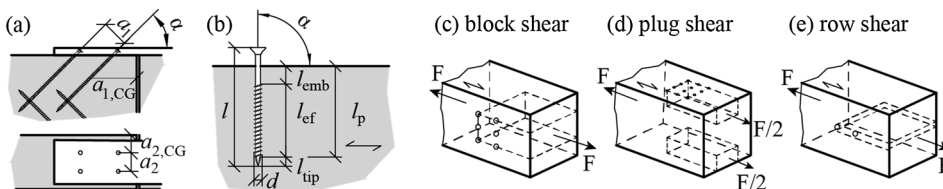


Fig. 2. (a) Spacing, end and edge distances according to EC 5 [3]; (b) geometric parameters of a single screw; (c), (d) and (e) shear failure mechanisms of laterally-loaded dowel-type fasteners anchored in timber.

dimension defined by the outer circumference of a part or the whole group of fasteners in a joint. Such quasi-brittle failure mechanisms are only possible in cases of combined tension and shear failures, indicating that the volume of timber enclosing the anchored group of fasteners is too small to achieve group withdrawal or screw steel failures instead. Although the wording for these failure mechanisms is similar to groups of laterally-loaded dowel-type fasteners, the failure characteristics are significantly different. For a clear definition, we briefly summarize the state-of-knowledge for laterally-loaded groups before discussing in detail specifics of block shear failure mechanisms of axially-loaded groups of screws.

1.4.2. Laterally-loaded dowel-type fasteners

In case of laterally-loaded groups of dowel-type fasteners block, plug and row shear failure mechanism may occur in cases where the timber elements are loaded parallel to the grain. These local, quasi-brittle timber failure mechanisms are characterized by failures of shear and tension parallel to grain planes enclosing the groups of fasteners; see Fig. 2(c)–(e). Depending on the penetration depth of the fasteners and their spacing perpendicular to the grain, differentiation can be made in (c) block shear (tearing-out of a timber block, in height equal to the entire structural element thickness), (d) plug shear (tearing-out of a timber block, in height below the entire element thickness) and (e) row shear (tearing-out of a timber block, comprising a row of fasteners in grain direction).

Simple models for these failure modes are for example provided in Foschi and Longworth [12] and EC 5 [3] (Appendix A) which consider the resistance of either the shear or the tension plane. In contrast, Kangas and Vesa [13] and Stahl et al. [14] take into account the sum of the resistance of the shear and tension planes. Recently, Zarnani and Quenneville [15] formulated an approach based on parallel acting springs, representing the potential shear and tension parallel to grain failure planes.

1.4.3. Axially-loaded dowel-type fasteners: focus self-tapping screws

In the case of primary axially-loaded groups of self-tapping screws, the block shear failure mechanisms comprise shear, rolling shear and tension perpendicular to grain failure planes. The superposition of forces induced by each screw in the group provokes a simultaneous or successive failure of the lateral and bottom failure planes encasing the timber block in which the screws are anchored. In contrast to laterally-loaded dowel-type fasteners, block shear failure does not lead to a tearing-out of a complete timber block. This is because of the residual resistance of timber after reaching the shear capacity in the transverse plane perpendicular to the grain (related shear strengths: $f_{v,RL}$ or $f_{v,TL}$, with subscripts L, R and T for longitudinal, radial and tangential fibre direction, respectively), where fibres are still active in bending and tension parallel to grain; see Jöbstl et al. [16] and Brandner and Dietsch et al. [17]. As block shear and related failure mechanisms in axially-

and laterally-loaded dowel-type fasteners are different, a clear differentiation and thus a definition and characterization for axially-loaded dowel-type fasteners is needed. In the following explanations, “pure block shear failure mechanism” (B1; see Fig. 3 left) is characterized by clearly visible cracked rolling shear and tension perpendicular to grain planes at the circumference of the group of axially-loaded screws. Deviating crack patterns, for example additional cracks caused by failures of rolling shear plane along each screws row in grain (Fig. 3 middle), additional cracks caused by failures of tension perpendicular to grain planes along the anchored thread (Fig. 3 right) or only partly existing cracks along mentioned potential failure planes are summarized to the “combined block shear failure mechanism” (B2).

So far, a design procedure for calculating the resistance of axially-loaded groups of screws in case of block shear is neither available nor considered in regulations regarding the minimum spacing, end and edge distances.

In analogy to the approach for block shear in laterally-loaded groups of fasteners from Zarnani and Quenneville [15] the following block shear model was established; see Mahlkecht et al. [7] and [8].

2. Block shear model

We now introduce briefly the block shear model of Mahlkecht et al. [7] and [8], defined for a thread-fibre angle $\alpha = 90^\circ$. It is based on a system of parallel acting linear-elastic springs representing deterministically the shear, rolling shear and tension perpendicular to grain properties of the corresponding failure planes. Free deforming timber surfaces are assumed. Constrained equal deformations of all failure planes cause that the failure plane with the highest stiffness attracts the highest share of the total load. Hence, the geometrical dimensions of the failure planes encasing the theoretical load-bearing volume are one of the key parameters in the model. Consequently, in addition to the spacing in and perpendicular to grain also the penetration length l_p of the group of screws influence the resistance against block shear failure; see Fig. 4.

Either one of the commonly acting lateral planes loaded in shear or rolling shear, or the bottom plane near the screw tips loaded in tension perpendicular to the grain can be the first failed plane(s), i.e. that failing plane(s) reaching its (their) maximum load-bearing capacity(ies) at first. Until then, load sharing amongst all potential failure planes, proportional to their individual stiffness, is assumed. Their stiffness values are defined as

$$\begin{aligned} K_{t,90} &= \frac{E_{t,90} A_{t,90}}{C_{t,90} l_p}; \quad K_s = \frac{G_0 A_{s,s}}{X_s} + \frac{E_{t,90} A_{t,s}}{10 l_p} \quad \text{and} \quad K_r \\ &= \frac{G_r A_{s,r}}{X_r} + \frac{E_{t,90} A_{t,r}}{10 l_p} \end{aligned} \quad (1)$$

with $K_{t,90}$, K_s and K_r as the stiffness values assigned to the bottom plane stressed in tension perpendicular to grain, for one lateral plane in shear

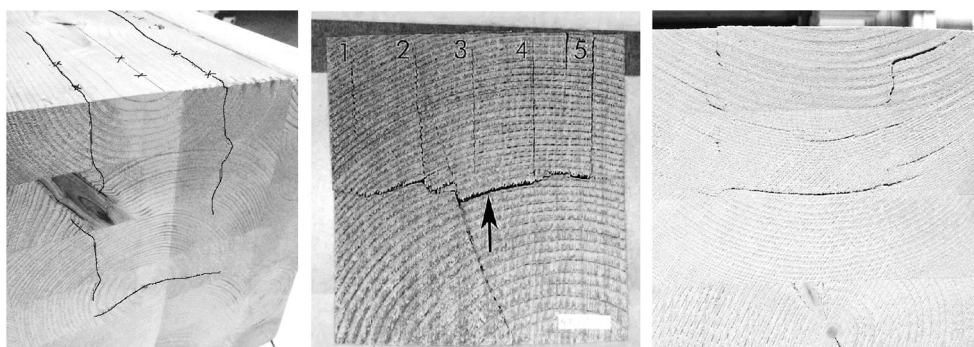


Fig. 3. (left) Pure block shear failure mechanism B1; (middle & right) combined block shear failure mechanism B2.

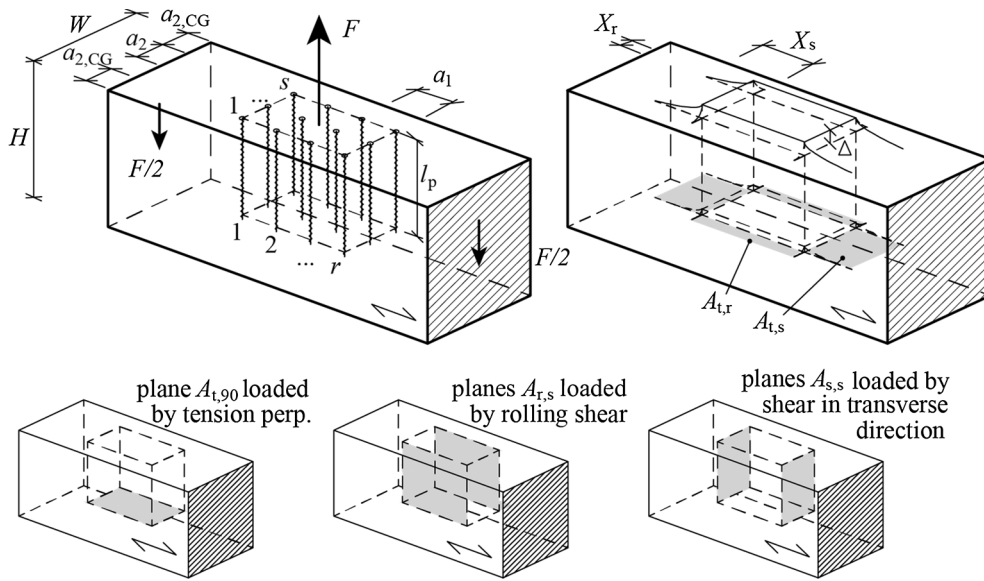


Fig. 4. Schematic representation of the block shear failure mechanism at $\alpha = 90^\circ$: definitions and geometric parameters; see Mahlkecht et al. [7] and [8]

and for one lateral plane in rolling shear, respectively. Hereby, $E_{t,90}$ is the modulus of elasticity for tension perpendicular to grain, G_0 and G_r are the shear modulus in transverse direction and rolling shear, respectively, $A_{t,90}$ is the area loaded in tension perpendicular to grain, $A_{s,s}$ and $A_{s,r}$ are the areas per lateral plane loaded transverse in shear and rolling shear, respectively, $A_{t,s}$ and $A_{t,r}$ are the bottom areas per lateral volume affected by adjacent shear in transverse direction and rolling shear, respectively, l_p is the penetration depth, $C_{t,90}$ the stress shape parameter (ratio of non-constant to constant stress distribution integrated over l_p), and X_s and X_r are the length and width of the affected adjacent transverse and rolling shear volume, respectively.

A successive failure curve is shown in Fig. 5. Load-elongation curves with theoretical single stiffness values K_1 , K_2 and K_3 give the ranked elongations $\epsilon_{f,(i)}$ with (i) as index for the ascending order, given as

$$\epsilon_{f,(i)} = f_i A_i C_i / K_i \quad (2)$$

with f_i as the corresponding strength value ($f_{t,90}$, f_v or f_r), A_i as the corresponding area ($A_{t,90}$, $A_{s,s}$ or $A_{s,r}$) and C_i as the corresponding stress shape factor (C_t , C_s or C_r). Until the first failure, all failure planes act together, with $K_1 + K_2 + K_3$. The elongation at the first partial failure, i.e. at the load level, denoted as F_{1st} , where the first plane(s) fail, is denoted as $\epsilon_{f,(1)}$. After this first failure, global (uniform) load redistribution between all remaining failure planes is assumed. The actual stiffness is then given as sum of the stiffness values of the remaining active planes. The load is increased until the next partial failure occurs.

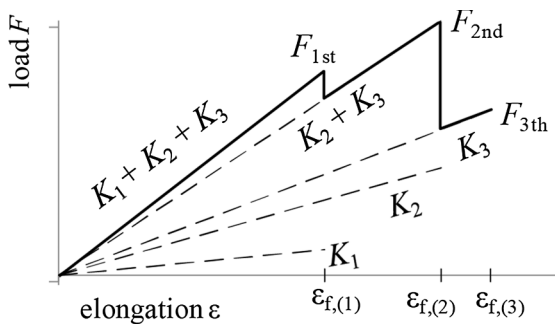


Fig. 5. Schematic representation of the block shear load-elongation curve as consequence of a successive failure process in case of linear-elastic behaviour.

This process is continued until the last plane(s) failed. The maximum resistance against block shear, F_{max} , is thus given as the maximum capacity reached during this successive failure process, see

$$F_{max} = \max_a \left[\sum_{j=a+1}^3 K_j \epsilon_{f,(j)} \right], \text{ with } a = 0, 1, 2 \quad (3)$$

Thereby a is the number of already failed (pairs of) planes.

The mechanical model requires 19 input parameters in total: seven for the geometry (spacing a_1 & a_2 , edge distances $a_{1,CG}$ & $a_{2,CG}$, number of rows r and columns s of screws in the group and penetration depth l_p), six material properties (three elastic constants $E_{t,90}$, G_0 & G_r and three strength properties $f_{t,90}$, f_v & f_r) and six stress shape parameters (coefficients $C_{t,90}$, C_t , C_s , C_r , and dimensions X_r & X_s). Apart from the well-defined geometrical parameters, for material and stress shape parameters a more detailed discussion is required; see the following Section 3. The parameters are analysed based on literature, own data and observations and by using analogies to existing mechanical models.

3. Setting of model parameters

The high number of model parameters necessitates a sound setting and background to get confidence on each value. The aim is to discuss each parameter and meaningful associated bandwidths, to outline related uncertainties and to validate the model for an agreed setting of parameters by using test data from Plieschounig [4], Mahlkecht [5], Mahlkecht and Brandner [6] and Mahlkecht et al. [7] and [8].

3.1. Geometric parameters

The design of groups of screws is currently determined by the spacing a_1 & a_2 as well as the end and edge distances $a_{1,CG}$ & $a_{2,CG}$, respectively. Knowing in addition the number of rows, r , (number of screws in direction perpendicular to grain) and columns, s , (number of screws in direction parallel to grain) as well as the penetration depth, l_p , the dimensions of all potential failure planes encasing the group of screws are defined.

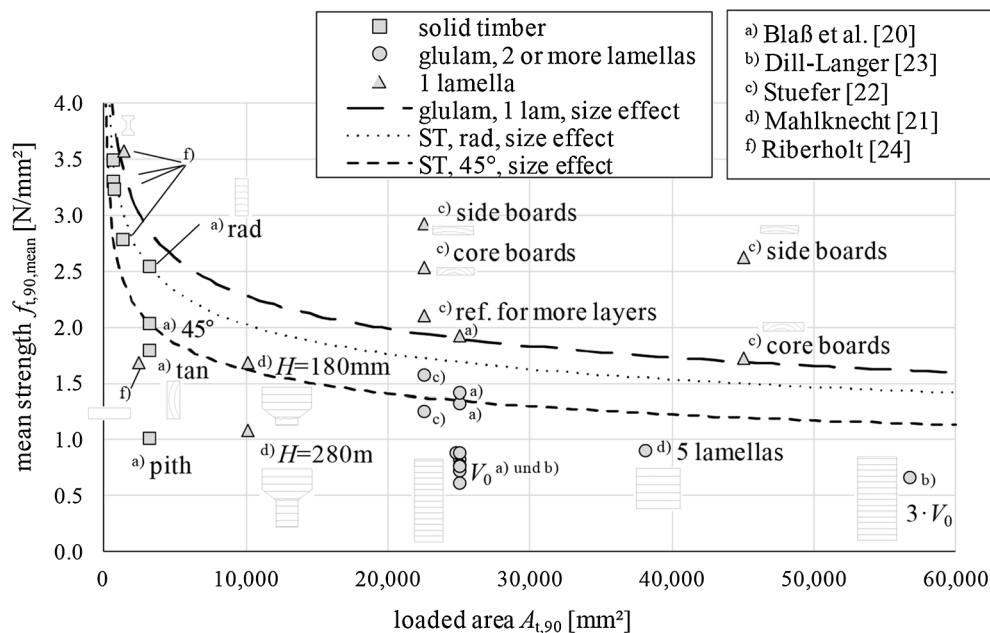


Fig. 6. Tension perpendicular to grain strength $f_{t,90}$ vs. loaded area $A_{t,90}$: solid timber (ST) and glulam (GLT).

3.2. Material parameters

3.2.1. General comments

Herein investigations are restricted to Norway spruce (*Picea abies*) and nominal strength classes C24 for solid timber according to EN 338 [18] and GL 24 h for glulam according to EN 14080 [19]. The material parameters, in particular strength values, needed here have to be representative for the specific loading situation and the small dimensions, areas and volumes involved. Both strength values, tension perpendicular to grain and shear, feature remarkable volume effects, i.e. a significant dependence of the element strength on the element volume. Furthermore, their relationship with density, as common indicator for other timber strength and elastic properties, is also poor. The following discussion aims on reliable settings for both properties.

3.2.2. Tension perpendicular to grain

Fig. 6 summarises investigations on tension perpendicular to grain strength, determined on various softwood species, specifically on clear wood (CW), solid timber (ST), board sections from lamellas (lam) and glulam (GLT), with reference to Blaß et al. [20], Mahlkecht et al. [21], Stuefer [22], Dill-Langer [23] and Ribberholt [24].

Properties in tension perpendicular to grain are one of the weakest properties of timber. They are mainly influenced by the sawing pattern (core boards from the centre vs. side boards from the outer part), the presence of pith and other timber growth characteristics as well as the timber product they refer to. Volume or size effects are frequently modelled as power models, with power parameter k . As in block shear tension perpendicular to grain failures typically occur at the screw tips, the interest is on the dependency of the strength value on the dimension of stressed area. This can be formulated as $f_{t,90} = f_{t,90,ref} (A_{t,90,ref}/A_{t,90})^{1/k}$, with $f_{t,90,ref}$ and $f_{t,90}$ as (reference) tension perpendicular to grain strength, $A_{t,90,ref}$ and $A_{t,90}$ as (reference) areas loaded in tension perpendicular to grain, respectively. Typical values for k are within a range of 4.5–5.2, see e.g. Mau [25] and Barrett [26]. EC 5 [3] gives $k = 5$ which is also applied further and used in power models for solid timber stressed at 45° or radially in Fig. 6, with $f_{t,90,mean} = 2.04$ and 2.55 N/mm^2 at $A_{t,90} = 3150 \text{ mm}^2$, respectively, and for single glulam

lamellas, with $f_{t,90,mean} = 1.93 \text{ N/mm}^2$ at $A_{t,90} = 25,000 \text{ mm}^2$; see Blaß et al. [20].

Considering the predefined crack plane (at the screw tip), adequate values can be either derived from investigations on single lamellas as well as on solid timber. In this context, it is also worth noting that all specimens which failed in block shear were made of solid timber or glulam from commercial productions featuring common timber growth characteristics and common variation in sawing patterns. Considering this, for the strength the value of Blaß et al. [20] for primary 45° annual ring orientation together with a size effect correction and $f_{t,90,mean} = 1.0 \text{ N/mm}^2$ as a lower limit is further applied. The upper limit for glulam is equal to the resistance of single lamellas (predefined crack plane!), and for solid timber equal to the resistance found for radially applied load; see Blaß et al. [20]. Again, a size effect correction is taken into account; see Fig. 6.

With respect to the modulus of elasticity in tension perpendicular to grain, values from small clear wood specimen tested radially ($E_{t,90,R}$) and tangentially ($E_{t,90,T}$) are within 390 and 817 N/mm^2 ; see e.g. Neuhaus [27], Hörig [28], Kollmann and Cote [29], Carrington [30] or Stamer [31]. In case of a 45° annual ring orientation Görlacher [32] and Blaß et al. [20] give mean values between 160 and 300 N/mm^2 . Following this, for the block shear model applied on solid timber of strength class C24, $E_{90,mean} = 350 \text{ N/mm}^2$ according to EN 338 [18] is used, with 300 and 400 N/mm^2 as lower and upper limits, respectively.

For glulam, a modulus of elasticity representing a system of parallel acting layers within the block shear volume is needed. EN 14080 [19] provides a value of $E_{90,mean} = 300 \text{ N/mm}^2$ for softwood glulam, independent of the strength class. This value agrees well with the range of 250–350 N/mm^2 as calculated from vibration tests by Görlacher [32] and Fellmoser and Blaß [33], considering $E_{stat} \sim 0.95 E_{dyn}$, with E_{stat} and E_{dyn} as the modulus of elasticity determined in static and vibration tests, respectively, and a mean density of 400–460 kg/m^3 . Comparable outcomes can also be found for glulam BS11 and BS14 in Blaß et al. [20]. To conclude: for the block shear model applied on glulam, a mean value of $E_{90,mean} = 300 \text{ N/mm}^2$ is used, together with 270 and 330 N/mm^2 as lower and upper limits, respectively.

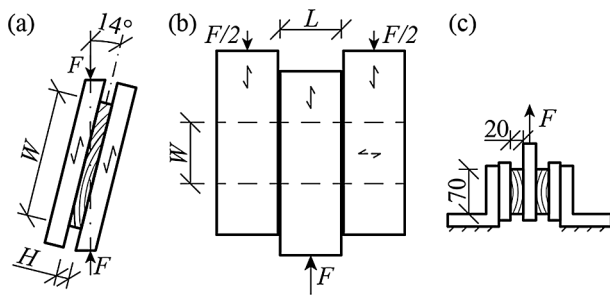


Fig. 7. Rolling shear test setups: (a) inclined; (b) in-plane three-point bending; (c) symmetric double-lap setup.

3.2.3. Rolling shear

The rolling shear strength f_r and the rolling shear modulus G_r are usually determined on specimens free of knots and knot clusters. Tests in literature comprise vibration tests (Görlacher [32]), inclined shear tests using an adapted setup from EN 408 [34] (see Mestek [35], Blaß and Flaig [36], Ehrhart [37] and Ehrhart and Brandner [38] and Fig. 7(a)), in-plane three-point bending tests (see Wallner [39] and Jöbstl et al. [16] and Fig. 7(b)), and shear tests using a symmetric double-lap setup (see Franzoni et al. [40] and Fig. 7(c)).

For solid timber, the rolling shear strength was found to be widely independent from the applied test setup and the sawing pattern, featuring mean values between $f_{r,mean} = 1.4$ and 2.1 N/mm^2 . For glulam, values for parallel acting lamellas are needed. In comparison to single lamellas, Ehrhart [37], for example, observed only a minor reduction of the mean rolling shear strength by testing up to four parallel acting board segments. For block shear, considering in addition the lateral deformation as being restricted by the lateral timber volume with thickness equal to $a_{2,CG}$, overall, only negligible influences on the mean rolling shear strength are expected. Hence, for the block shear model, the same mean value $f_{r,mean}$ for solid timber and glulam can be applied. In view of common dimensions of investigated girders featuring block shear failures, a reduced rolling shear resistance because of tension stresses perpendicular to the grain on free edges, as it occurs when testing single lamellas, is not taken into account. Comparing the densities and sawing patterns as found in our tests with that in Ehrhart and Brandner [38], for the block shear model a mean rolling shear strength of $f_{r,mean} = 1.90 \text{ N/mm}^2$ is seen as appropriate, with 1.4 and 2.1 N/mm^2 as upper and lower limits, respectively.

The rolling shear modulus G_r depends on the annual ring orientation and is maximal at 45° and minimal at 0° and 90° . For Norway spruce and specimens featuring nearly homogeneous sawing patterns, theoretically values between 50 and 350 N/mm^2 are possible; see Jakobs [41] and Görlacher [32]. Numerical investigations on common cross sections of side and core boards in Aicher and Dill-Langer [42] give values of 133 and 88 N/mm^2 , respectively. By testing small clear wood specimens (Bendtsen [43], Neuhaus [27] and Carrington [30]) and board segments (Görlacher [32], Fellmoser and Blaß [33], Blaß and Flaig [36], Ehrhart and Brandner [38] and Franzoni et al. [40]) mean values between 40 and 140 N/mm^2 are found. For the block shear model, based on Ehrhart and Brandner [38] a mean value of $G_{r,mean} = 100 \text{ N/mm}^2$ and 60 and 140 N/mm^2 as limiting values are applied.

3.2.4. Shear in transverse direction

The shear strength of timber in transverse direction, $f_{v,RL}$ and $f_{v,TL}$, is hard to determine. Due to the duality of shear stresses and the radial anisotropy of timber, shear failures commonly occur along LT and LR planes, with corresponding shear strengths $f_{v,LR}$ and $f_{v,LT}$, respectively. Analogies are possible to recent investigations conducted on single nodes and non-edge bonded CLT diaphragms composed of orthogonal-

layered lamellas. In such elements, a so called net-shear failure mechanism can occur which is characterized by local longitudinal shear failures along the boundaries between annual growth rings over the whole lamella cross section, in combination with local torsion failures at the edges of the rectangular gluing interface between the orthogonal layers. The local longitudinal shear failures lead to dissolution of fibre contact and in series arise small double-sided fixed cantilevers, stressed in bending and tension parallel to grain; see Jöbstl et al. [16], Hirschmann [44], Brandner et al. [45] and Brandner and Dietsch et al. [17] and Fig. 8.

The resistance of timber failing in net shear with according to these references, mean values between 6 and 14 N/mm^2 are reported, which are significantly higher than in longitudinal shear (see Spengler [46], Müller et al. [47] or Schäfers [48]). Apart from differences in the failure mechanism, the reason for the higher shear strength in CLT is also because of a distinctive locking effect in thin layers, caused by restraining effects of adjacent orthogonal layers, which is also responsible for a significant size effect in respect to the lamella thickness, with power coefficient $1/k = 0.4$. With respect to investigations on size and volume effects on longitudinal shear in solid timber and glulam (e.g. Brandner et al. [49]), half of this power coefficient can be dedicated to the locking effect and half to the structural size effect, as relevant for the block shear failure plane, whereby the structural size effect for solid timber (ST) and glulam (GLT) can be described as (Brandner et al. [49])

$$f_{v,mean,ST} = 55.2 A_{s,s}^{-0.22} \quad (4)$$

and

$$f_{v,mean,GLT} = 40.2 A_{s,s}^{-0.20} \quad (5)$$

with $A_{s,s}$ as shear area, see Fig. 4.

For the latter presented block shear tests and according to Eqs. (4) and (5), mean values $f_{v,mean} = 5.8$ and 8.6 N/mm^2 can be found on a conservative basis, with 5.0 N/mm^2 as a lower limit for both, and 8.0 and 9.0 N/mm^2 as upper limits for glulam and solid timber, respectively.

For the shear modulus, the same values as known for longitudinal shear can be used. Small clear wood specimens tested in Högig [28], Neuhaus [27] and Müller et al. [47] featured mean values between 540 and 775 N/mm^2 . EN 338 [18] regulates $G_{0,mean}$ for solid timber and strength class C24 or T14 with 690 N/mm^2 . For glulam, EN 14080 [19] gives $G_{0,mean} = 650 \text{ N/mm}^2$ for all strength classes. This value was also confirmed by Blaß [50] and Brandner et al. [51] and [52] and by applying the regression model from Görlacher and Kürth [53] with $G_{0,mean} = 1.78 \rho_{mean} - 146$, which was derived from vibration testing of board segments. $G_{0,mean} = 650 \text{ N/mm}^2$ are also taken for the block shear model, together with 550 and 750 N/mm^2 as limits for both, solid timber and glulam.

3.2.5. Summary of material parameters

Table 1 summarizes mean values for strength and elastic properties together with limiting values as applied further in the block shear model. The influence of these parameter settings on the model is discussed later in Section 5.4.4, as part of a sensitivity analysis.

3.3. Load distribution properties

3.3.1. General comments and FEA specifications

Now we concentrate on the load and stress distribution along the shear failure planes (rolling shear and shear in transverse direction) as well as the failure plane in tension perpendicular to grain. In the block shear model presented in Section 2, a uniform stress distribution along these planes is assumed. In reality, non-uniform distributions are given, which in the model are considered by the coefficients $C_{t,90}$, C_t , C_s and

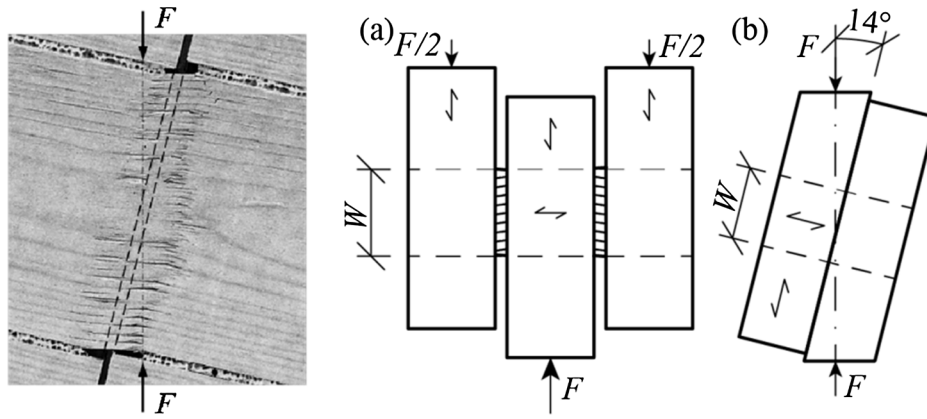


Fig. 8. (left) Net-shear failure pattern; (right) setups for testing net-shear failure mechanism: (a) symmetric (two shear lines) and (b) inclined (one shear line); Hirschmann [44] and Jöbstl et al. [16].

Table 1

Mean material properties and limit values for the block shear model; ST (C24 according to EN 338 [18]) & GLT (GL 24 h according to EN 14080 [19]) of Norway spruce (*Picea abies*).

Model parameters	Material	Setting (min mean max)
$f_{t,90,mean}$ [N/mm ²]	GLT	1.00 $2.04 \left(\frac{3,150}{A_{t,90}} \right)^{1/5}$ $1.93 \left(\frac{25,000}{A_{t,90}} \right)^{1/5}$
	ST	1.00 $2.04 \left(\frac{3,150}{A_{t,90}} \right)^{1/5}$ $2.55 \left(\frac{3,150}{A_{t,90}} \right)^{1/5}$
$E_{t,90,mean}$ [N/mm ²]	GLT	270 300 330
	ST	300 350 400
$f_r,mean$ [N/mm ²]	GLT & ST	1.4 1.9 2.1
$G_r,mean$ [N/mm ²]	GLT & ST	60 100 140
$f_v,mean$ [N/mm ²]	GLT	5.0 $40.2 A_{s,s}^{-0.20}$ 8.0
	ST	5.0 $55.2 A_{s,s}^{-0.22}$ 9.0
$G_{0,mean}$ [N/mm ²]	GLT	550 650 750
	ST	550 690 750

C_r . Furthermore, the effective widths of the additional lateral timber volume surrounding the group of screws and contributing to load-bearing are taken into account by the geometrical dimensions X_s and X_r . The dependency of the stress distribution coefficients from loading and supporting conditions has to be considered as well. Approximations discussed in the following are obtained (i) from stress distribution analysis on similar mechanical problems, (ii) by comparing test results with model outcomes applying different parameter settings and (iii) from a finite element analysis (FEA) conducted with the software

package RFEM 5.05.0018 (© Dlubal Software GmbH).

Ad (iii), the following numerical investigations are based on a beam representing one column of the total group of screws inserted, which is in width equal to a_2 , in depth equal to the original beam, and exposed to a two-dimensional stress state, see Fig. 9 (left).

This representative beam is modelled as a two-dimensional plane with linear-elastic orthotropic material properties either for GL 24 h according to EN 14080 [19] or for C24 according to EN 338 [18]. The geometric dimensions of the beam, the number of screws and the distance between group and support are varied. The support is modelled as a line of springs at the upper side (“push-pull” test setup), only active in compression and featuring a stiffness in z-direction of $C_{u,z} = 300,000$ kN/m² multiplied by a_2 . The screws are also modelled as planes with properties representing steel. Only the upper flanges of the screw thread, represented by the upper line of the triangles on both sides of the steel planes, feature a rigid contact with the surrounding timber surface; all other steel plane contact lines are modelled without contact to timber, i.e. without possible load transfer; see Fig. 9 (right). Loading of the group of screws is modelled in two different ways: (I) directly, via a line load applied directly on the top of each screw, and (II) indirectly, via a line load applied on an additional thick (rather stiff) steel plane, representing a steel plate commonly used for load introduction in testing groups of screws, connected to all screws in the group but without contact to the timber plane, see Fig. 10. Whereas approach (I) mirrors a group of screws each with an equal load, approach (II) ensures (widely) equal displacements, providing the upper steel plate and the timber beam are stiff enough ($E I \rightarrow \infty$). Approach (II) corresponds widely to the test setups used in our investigations.

3.3.2. Stress shape parameter $C_{t,90}$

There is only limited information on the stress distribution along the

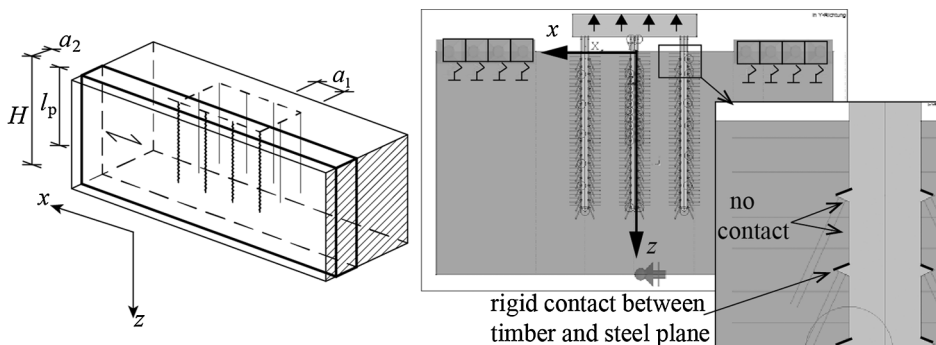


Fig. 9. (left) Beam representing one column of a group of screws; (right) principle model applied in FEA.

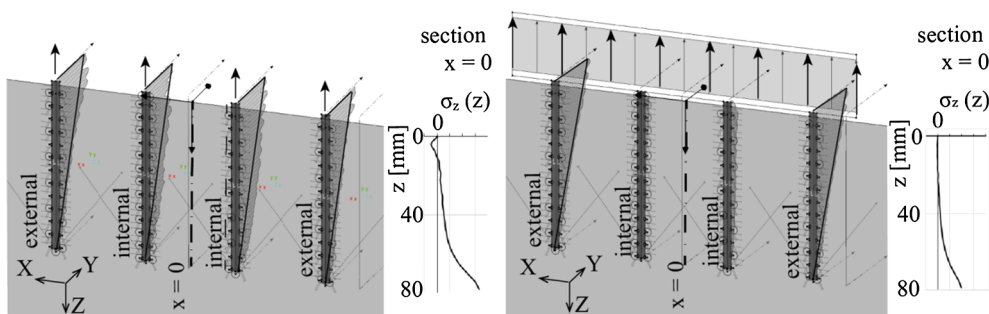


Fig. 10. Distribution of stress σ_z along external and internal screw threads and in the surrounding timber: (left) equal load on each screw (I); (right) equal displacement of each screw (II).

threaded-part of axially-loaded screws anchored in timber. Ehlbeck and Sibert [54] as well as Ringhofer and Schickhofer [55] report on a minor concave, non-linear force distribution. In herein conducted FE-model, along the external screw (screw on the edge of the group) an approximate linear stress distribution is observed. The internal screws (screw in the middle of the group) feature a different stress distribution which depends on the applied loading approach, i.e. imposed equal loads (I) or equal displacements (II); see Fig. 10. In case of external screws the forces induce tension stresses in timber parallel and perpendicular to grain, within the group of screws, as seen for the internal screws, the stress components perpendicular to the grain collide. In fact, a clear convex stress distribution along the internal screws is observed. In case of imposed equal loads (I), see Fig. 10 (left), the maximum values of external and internal screws are equal. However, in case of imposed equal displacements (II) the external screws have to bear significantly more load than the internal screws, see Fig. 10 (right).

According to “actio” = “reactio”, the stress distribution in timber has to be contrary to the screws, accumulating the inserted stresses. Irrespective of the applied loading approach, the stresses in timber, from top ($x_{\text{global}} = 0$) to l_p , increase exponentially. This non-linearity even increases with increasing end and edge distances of groups of screws and supports. However, the stress distribution converges to linearity when the spacing between the screws increases. Hence, for the coefficient $C_{t,90}$, defined as ratio between a non-uniform versus a uniform stress distribution integrated over l_p of the volume teared-out in case of block shear failure, values between 0.3 (non-linear) and 0.5 (linear) can be determined.

In the tests described in Section 4, for loading the groups of screws, rigid steel plates were applied, which corresponds qualitatively to Fig. 10 (right) and (II). Thereby, the external screws have to bear significantly more load than the internal screws; in numbers, approximately 75% of the total load is carried by the two external screws and approximately 25% by the two internal screws. However, this FE-analysis is based on a linear-elastic material behaviour. In reality, axially-loaded screws feature a significant non-linear elastic-plastic behaviour before reaching the maximum capacity followed by a non-linear softening. Thus, axially-loaded group of screws in reality have a certain potential to redistribute loads. To prove this, a group of four screws was analysed by means of a probabilistic model, which has embedded a full-stochastic description of the non-linear load-displacement withdrawal behaviour of axially-loaded screws; see Brandner et al. [56]. In this model and according to the FEA, the external to internal screws are weighted at 3:1. Based on 1000 simulated groups of screws and by comparing the mean values $n_{\text{ef}} = 0.91$ was found which is rather close to the test outcomes as discussed later in Section 5.

For validating the proposed block shear model later, we assume a load redistribution between the three to five screws per column in tested groups of screws, see Section 4, and thus a linear stress distribution with $C_{t,90} = 0.5$. This value is, in analogy, conform to the

assumed linear tensile force distribution in a row of rivets in sheared dowel-type connections; see Zarnani and Quenneville [15].

By comparing the stress distributions along the anchored threaded part of screws with that in timber, by means of FEA and by analysing test setups with near and distant supports the influencing ratio of penetration length and beam height (depth), l_p/H , as well as differences in load configuration (equal loading vs. equal elongation) lead to parameter values $C_{t,90} = 0.3\text{--}0.5$. Overall, $C_{t,90} = 0.5$ is found to be suitable for both test setups discussed later on in Section 4.

3.3.3. Stress shape parameters C_b , C_r and C_s

Coefficients C_b , C_r and C_s allow adjusting the assumed uniform stress distribution to a more realistic non-uniform stress distribution by comparing the integrals of stresses over the failure planes. For the bottom plane $A_{t,90}$, dedicated to tension perpendicular to grain failure, for simplicity a uniform stress distribution is assumed, with $C_t = 1$. For the shear failure planes more comprehensive analyses are required.

FE-analyses on test setups used in our experimental investigations (see Section 4) reflect slightly non-uniform stress distributions in cases where the supports are close to the edge of the group of screws, which turned out to be independent from the depth of the timber member, with C_r and C_s approximately 0.8–0.9, see Fig. 11 (left). In cases of larger spacing a_1 , $C_r = C_s = 0.9$ applies. In Fig. 11 (left) the qualitative stress distribution is shown on the section “L-64” in the middle between the screw axis and the support, avoiding stress peaks near the stress field of the screw. For analogy, the same section is shown in Fig. 11 (right). The tested embedment lengths $l_{\text{emb}} = 2d$ and $4d$ were too short to significantly influence the stress distribution. Thus, for investigated partially- and fully-threaded screws, considering $l_p = l_{\text{ef}} + l_{\text{emb}}$ as depth of the block shear volume, the same values can be applied.

Investigations were also made on test setups featuring larger distances between joint and supports. For $l_p/H = 0.5$ a stress distribution along the shear failure planes, similar to the setups featuring near supports, was observed. However, in the case of $l_p/H = 0.7$, the stress distribution was rather uniform.

Finally, for test setups with near supports, $C_r = C_s = 0.9$, with 0.8 and 1.0 as limiting values, were chosen. For distant supports, $C_r = C_s = 1.0$, with 0.9 as a lower limit, are used.

3.3.4. Dimensions X_s and X_r

The dimensions X_s and X_r are the widths of material surrounding the group of screws in longitudinal and transverse direction, respectively, which additionally contribute in bearing transverse and rolling shear loads. So far, reliable values for these two parameters are missing and influences from varying support conditions expected.

In general, block shear failure is expected when the volume surrounding each individual screw in a group is too small, meaning that stresses of neighbouring screws accumulate, and the anchorage capacity of the inserted screws is higher than the resistance of the timber

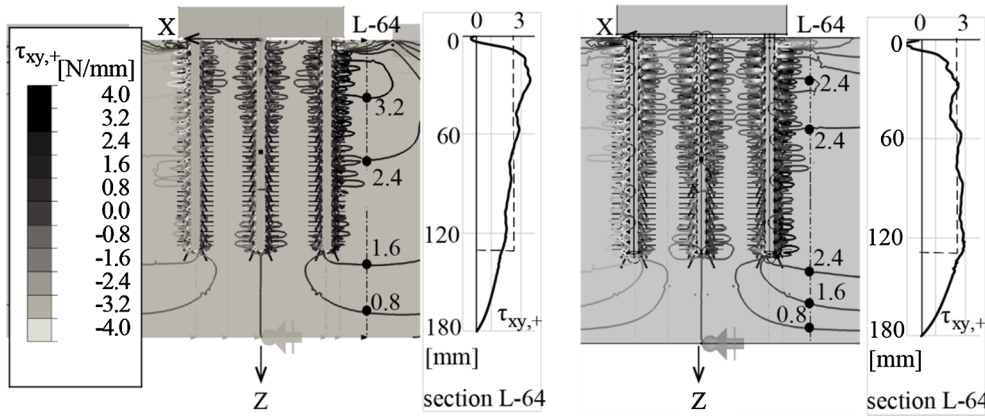


Fig. 11. Shear stress distribution along the lateral shear plane $A_{s,s}$ for $l_p/H = 0.7$ for near (left) and distant support (right).

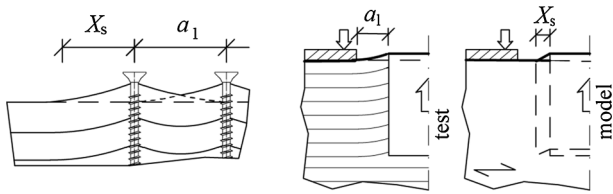


Fig. 12. (left) Overlap of zones influenced per screw; (centre and right) X_s exemplarily for a test setup featuring near supports.

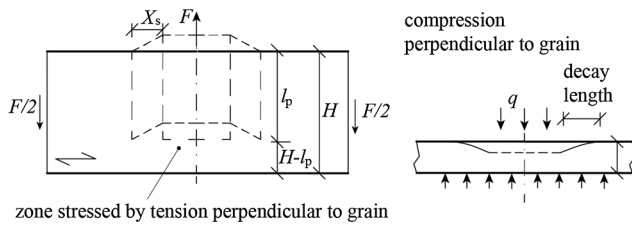


Fig. 13. Approach for determining the decay length of the zone stressed by tension perpendicular to grain (left) in analogy to compression perpendicular to grain models (right).

volume enclosed by the group of screws. The accumulation of screw forces is schematically shown in Fig. 12 (left) by overlapping cones of timber surrounding the screws. Consequently, X_s and X_r are assumed to be at least the half of the minimum spacing $\geq a_1/2$ and $\geq a_2/2$, respectively. X_s and X_r are determined by investigating the relationship between spacing a_1 and a_2 and correspondingly observed failure mechanism (see Section 4), i.e. sufficient spacing to achieve withdrawal and steel failures of screws. Furthermore, the influence of a near support, i.e. by limiting X_s by applying a_1 , as it occurred in some

investigated test setups (see Section 4) and as exemplarily shown in Fig. 12 (centre and right), is considered as well.

To discuss the dimensions X_s and X_r on a more fundamental basis, two-dimensional mechanical models describing analogue stress states as well as loading and support conditions are analysed. With a focus on the bottom plane, at first the elastic deformation in analogy to local compression perpendicular to grain models is analysed. The decay length in longitudinal direction, X_s , results from the elastic displacement of the theoretical surface at the bottom plane. The local compression perpendicular to grain models with rigid support at the opposite side are applied in some analogy to tension perpendicular to grain stresses, see Fig. 13. Madsen et al. [57] modelled fibres close to loading area, stressed in bending and shear, as beams on elastic foundations. According to Madsen et al. [57], the foundation modulus and the beam stiffness are given as $k = E_{90} a_2/(H - l_p)$ and $E_0 a_2 d^3/12$, respectively, with a_2 as width of the theoretical beam. Based on FEA, for the parameter beam depth Madsen et al. [57] found the relationship $d = 0.17 (H - l_p)$. Using this approach in analogy, in the case of block shear, the decay length in longitudinal direction X_s would be

$$X_s \cong 3 (4 E_0 I/k)^{1/4} = 0.60 (H - l_p) \left(\frac{E_0}{E_{90}} \right)^{1/4} \quad (6)$$

with E_0 and E_{90} as moduli of elasticity parallel and perpendicular to grain, respectively, and I as moment of inertia.

Similar analysis on the embedment of an orthotropic timber beam is done by Tanahashi et al. [58]. The shape of the displacement is the outcome of an elastic surface analysis. The plastic components of the model formulated in the stiffness functions can be excluded. The displacement w of the lateral surface follows an exponential decrease $e^{-\gamma|x-L|}$ with $L = 0.5 (r - 1) a_1$ and the characteristic value γ , which is based on the elastic properties (modulus of elasticity E , shear modulus G and Poisson's ratio ν). We define the decay length per notation as a

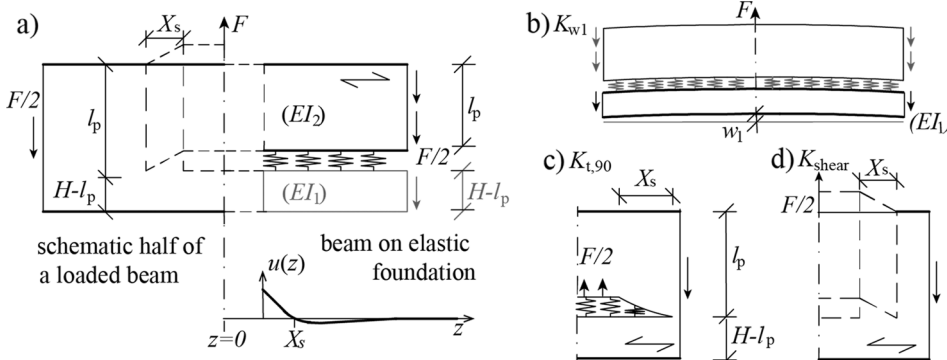


Fig. 14. (a) Schematic representation of one half of a tested group of axially-loaded screws failing in block shear and one half of the schematic model of Barber [60] for a beam on elastic foundation; springs representing (b) the bending stiffness of part "1", (c) tension perpendicular to grain stiffness at the bottom plane and (d) shear flow along the surrounding shear planes.

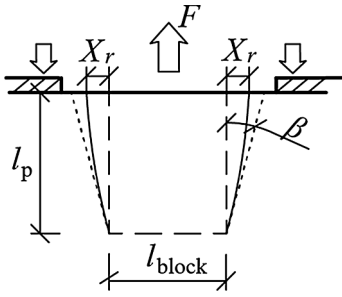


Fig. 15. Load spreading model from Van der Put [62] exemplarily adapted for estimating the width X_r .

distance between the shear failure planes until a residual lateral upper surface deformation of 1%, measured from the sole lateral deformation of the whole timber block surrounding the screws. Hence, X_s can be estimated as

$$X_s \cong -\ln(0.01) (H - l_p) / (\gamma(H - l_p)) \quad (7)$$

For the factor $\gamma(H - l_p)$ and Japanese Yellow cedar Tanahashi et al. [59] gives a range of 2.3–3.0 for the planes LR, LT and LTR. As the ratio E_0/G_0 for Norway spruce and Japanese Yellow cedar is comparable, we apply the same range also in our investigations.

By applying the approaches of Madsen et al. [57] and Tanahashi et al. [58], the outcomes for X_s are rather close and allow to use $X_s \cong 1.6 (H - l_p)$. Finally, both approaches result in a linear relationship of $X_s/(H - l_p)$, which is, however, suitable only for height $H - l_p$ of a few centimetres.

The length X_s can be also investigated in analogy with the decay length in beams loaded locally in tension perpendicular to grain. Barber [60] proposed a model for a semi-infinite beam on linear-elastic foundation. This beam is loaded at the symmetrical axis with the force F , see Fig. 14(a). By adapting this model to represent one half of the timber block which is torn-out in case of a block-shear failure, another mechanically based approximation for the width X_s can be found as the distance stressed in tension perpendicular to grain. The overall stiffness is the stiffness of three springs in parallel. The first stiffness is $K_{w1} = 1/w_k$, representing the bending stiffness of the theoretically separated residual beam with cross section $(H - l_p) a_2$ and length l . The second stiffness, $K_{t,90}$, considers the elongation along the zone stressed in tension perpendicular to grain. The third stiffness describes the shear stiffness K_{shear} of the theoretically separated beam with cross section $l_p a_2$ and length X_s ; see Eq. (8) and Fig. 14.

$$K_{tot} = K_{w1} + K_{t,90} + K_{shear} = \frac{24 \pi (E_0 I_1)}{l^3} + \frac{E_{t,90} X_s a_2}{10 (H - l_p)} + \frac{G_0 l_p a_2}{X_s} \quad (8)$$

The deflection $u(z)$, given as

$$u(z) = -\frac{2 \beta F/2}{K_{tot}} e^{-\beta z} \cos(\beta z), \quad \text{with } \beta = \sqrt[4]{\frac{K_{tot}}{4 (E_0 I_2)}} \quad (9)$$

depends on the parameter β , which itself depends on the spring stiffness K_{tot} and the bending stiffness $(E_0 I_2)$ of the theoretically torn-out timber block, with cross section $l_p a_2$. $u(z) = 0$ defines the distance at which the stresses perpendicular to grain change from tension to compression, allowing to evaluate $X_s = \pi/(2 \beta)$, see Fig. 14.

In addition also the models of Ehlbeck and Görlacher [61] and Stahl et al. [14] were investigated and adopted, however without success.

Finally and again in analogy to local compression perpendicular to grain stresses, the load spreading model of Van der Put [62] is adapted; see Fig. 15. The coefficient $k_{c,90}$, which is defined as $k_{c,90} = f_{c,90,partial}/f_{c,90,full}$, with $f_{c,90,partial}$ and $f_{c,90,full}$ as the compression perpendicular to grain strengths (defined per notation) of partially (concentrated) and fully distributed loads (complete surface uniformly loaded and supported), respectively, is based on a non-linear load spreading over the depth l_p . For bending members exposed to compression perpendicular to grain Leijten et al. [63] proposed to limit the depth dedicated to stress dispersion by $\min(0.4H; 140 \text{ mm})$. Following this, the dimension X_s but also X_r can be estimated as

$$X_s \text{ and } X_r = 0.5 l_{block} (k_{c,90} - 1) \quad \text{with } k_{c,90} = \sqrt{\frac{l_{block} + 2 l \tan \beta}{l_{block}}} \leq 5 \text{ and } l = \min(l_p; 140 \text{ mm}) \quad (10)$$

According to Van der Put [62] and Brandner and Schickhofer [64], for spreading parallel (relevant for X_s) and perpendicular to grain (relevant for X_r), in the elastic range the angle β can be assumed with 45° and 15° , respectively. The block lengths in longitudinal and transverse direction are defined as $l_{block} = (r - 1) a_1$ and $l_{block} = (s - 1) a_2$, respectively, see Fig. 15.

With the mechanical model approaches, a range for length X_s and X_r can be found. As already mentioned, the conclusion of $X_i \geq a_i/2$ for investigated samples with block shear failure mechanism and consequently $X_i \leq a_i/2$ for other observed failure mechanisms is done later in Section 5.3.

4. Experimental investigations

4.1. General comments

For testing axially-loaded groups of screws, two different setups were developed; these are described in more detail in the following. In both setups a group of $n = r s$ self-tapping screws were inserted without pre-drilling and at a thread-grain angle of $\alpha = 90^\circ$. The groups of screws, loaded by force F axially in tension, were tested by means of a

Table 2
Overview: tested series and main parameters.

Series [-]	Main parameters [-] ^a
s'10	Test setup T1: circumferential support; PT 6 × 300/75 ($l_{ef} = 11.3 d$, $l_{emb} = 2 d$) ST C24, $\rho_{12,mean} = 430 \text{ kg/m}^3$ (CV = 10.8%), $u_{mean} = 13.1\%$ (CV = 3.2%)
s'11	Test setup T1: circumferential support; PT 6 × 300/163 ($l_{ef} = 25.7 d$) & PT 6 × 300/75 ($l_{ef} = 11.3 d$, $l_{emb} = 4 d$) ST C24, $\rho_{12,mean} = 404 \text{ kg/m}^3$ (CV = 9.4%), $u_{mean} = 14.4\%$ (CV = 7.9%)
s'12	Test setup T1: circumferential support; PT 6 × 420/163 ($l_{ef} = 28.3 d$, $17.8 d$, $14.2 d$) Glulam GL 24 h, $\rho_{mean} = 453 \text{ kg/m}^3$ (CV = 3.3%), $u_{mean} = 11.6\%$ (CV = 2.8%)
s'15	Test setup T1: longitudinal support; FT 8 × 180 ($l_{ef} = 8.8 d$) and FT 8 × 280 ($l_{ef} = 24.8 d$) Glulam GL 24 h, $\rho_{12,mean} = 406 \text{ kg/m}^3$ (CV = 3.8%), $u_{mean} = 11.3\%$ (CV = 5.8%)
f'13	Test setup T2: single span girder; FT 8 × 180 ($l_{ef} = 18.5 d$) and FT 8 × 280 ($l_{ef} = 31.2 d$) $H_{cs} = 180 \text{ mm}$: glulam GL 24 h, $\rho_{12,mean} = 461 \text{ kg/m}^3$ (CV = 5.4%), $u_{mean} = 12.7\%$ (CV = 2.8%) $H_{cs} = 280 \text{ mm}$: glulam GL 24 h, $\rho_{12,mean} = 428 \text{ kg/m}^3$ (CV = 3.9%), $u_{mean} = 12.5\%$ (CV = 2.1%)

^a PT ... partially-threaded screw; FT ... fully-threaded screw. ST ... solid timber acc. to EN 338 [18]; GLT ... glued laminated timber (glulam) acc. to EN 14080 [19].

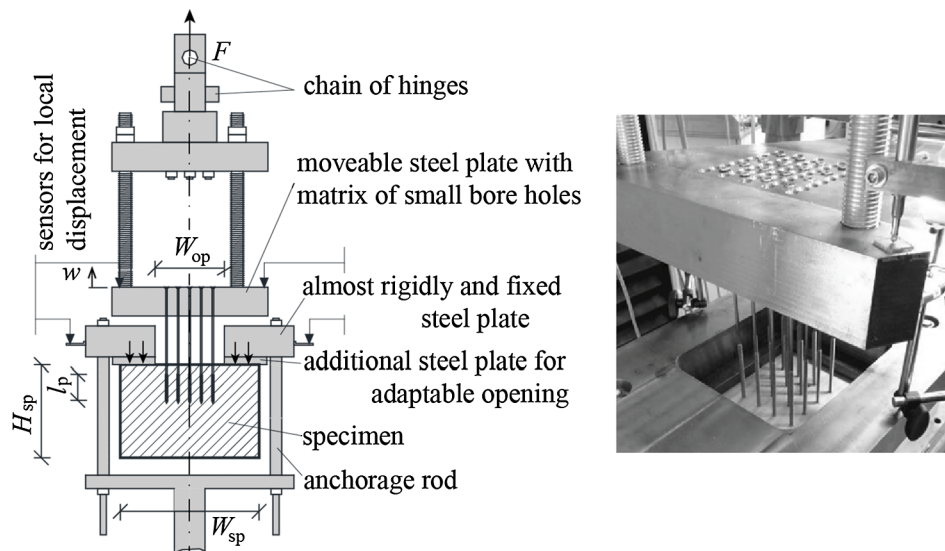


Fig. 16. Test setup T1 with circumferential support; (left) schematically and (right) as executed.

“push-pull” test setup. To investigate different failure mechanisms and influences on resistance, in both test setups spacing in and perpendicular to grain, a_1 and a_2 , respectively, and penetration length, l_p , were varied. In the following, resistances and failure mechanisms of all groups tested in solid timber and glulam of Norway spruce (*Picea abies*) are presented and compared with the outcomes of corresponding single screw tests.

4.2. Material, test setups and variations

4.2.1. Overview

Table 2 shows a compilation of tested series and main parameters. In total, five test series (s'10, s'11, p'11, s'12 & s'15) investigated groups of screws featuring a near support test setup. One series (f'13) was used to analyse the group behaviour in the case of distant supports.

The following outlines the main characteristics of the different test setups used for investigating the five different test series. Details on specimen geometry, screw insertion, group arrangement and number of tests, together with test outcomes and failure modes, are presented in Table 5 (series s'10, s'11, s'12 & s'15) and Table 6 (series f'13) in the Appendix.

4.2.2. Test setup T1 – near support

Plieschoung [4] (series s'10) developed a setup for testing groups of screws in withdrawal analogue to single screw withdrawal tests according to EN 1382 [65], by loading the screws constantly and displacement controlled to reach F_{max} in 90 ± 30 s after pre-tensioning, which is described in the following. A circumferential support was chosen to minimize bending stresses. For test series s'11, see Mahlkecht [5], structural timber of nominal strength class C24 according to EN 338 [18] with cross section height H_{cs} and width W_{cs} was used. To increase the bending stiffness and to reduce the compression perpendicular to grain stresses, some of the specimens were reinforced laterally and at the bottom by means of additional, glued-on structural timber and CLT elements. Specimens characterized in geometry by height H_{sp} , width W_{sp} and length L_{sp} , were positioned beneath a stiff steel plate fixed in its position with a rectangular opening in the centre. The dimensions of the opening length L_{op} and width W_{op} were adapted according to the required test setup by means of additional steel plates. Instead of the rectangular opening, one of these additional steel plates featured a matrix of small bore holes allowing an investigation of

different groups of screws mirroring a restricted surface deformation, i.e. comparable to groups of screws in steel plates compressed continuously on the timber surface while loaded axially, so-called “restricted joints”. Screws of nominal diameter $d = 6$ mm were inserted through a second stiff steel plate, positioned with degrees of freedom in vertical and horizontal direction and featuring a bore hole matrix for testing different group sizes and arrangements, i.e. different spacing, see Fig. 16. To ensure that all screws in a group are loaded and equally elongated, each screw was repeatedly pre-tensioned manually applying a torque moment of 6 Nm by means of a torque wrench. This pre-tensioning phase was recorded continuously. During testing, local displacements were measured in the middle at both side lengths of the fixed steel plate and at the three edge points of the upper moveable steel plate.

For test series s'12, which is partially published in Mahlkecht et al. [7] and [8], industrially produced glulam of nominal strength class GL 24 h according to EN 14080 [19] was used. The test procedure was adjusted according to EN 26891 [66]. The advancing displacement rate was adapted according to the estimated maximum load of each sample.

In test series s'15 glulam produced in the laboratory was used featuring criteria for a nominal strength class GL 24 h according to EN 14080 [19] with the exception that lamellas without knots were preferred. The specimen had no additional reinforcement and only supported laterally on both end-grains but not at specimen side-lengths. Thus, additional bending stresses are significantly higher than in the other series. Self-tapping screws of three different producers (H1, H2 and H3), all of nominal diameter $d = 8$ mm, were tested. Advancing displacement rate was chosen as constant with 1 mm/min.

4.2.3. Test setup T2 – beam loaded perpendicular to grain

In the horizontal test setup T2, published by Mahlkecht et al. [7] and [8], a beam was centrally point-loaded and supported as a single span girder. The free span was limited by the testing machine and featured approximately 575 mm; see Fig. 17. In contrast to T1, in T2 additional significant bending stresses occurred. The specimen were of glulam of nominal strength class GL 24 h according to EN 14080 [19], excluding one sample reinforced laterally by glued-on structural timber elements. The axial load was applied centrally via a connecting steel plate, which allows a rectangular arrangement of the group of screws but no screws in the centre. The group arrangement is again defined by r and s as the number of screws in rows parallel and columns

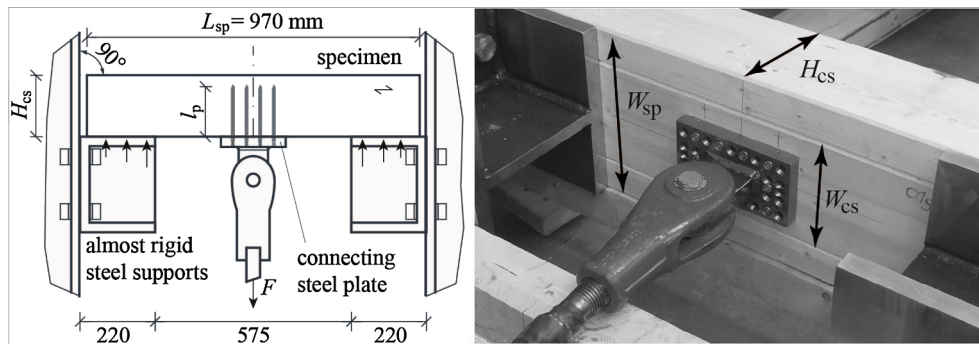


Fig. 17. Test setup T2 with single span girder (left) schematically test setup and (right) view on test setup.

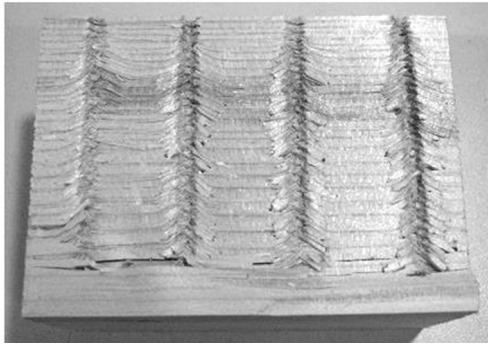


Fig. 18. Typical plastic fibre deformation pattern in case of withdrawal failure mechanism.

perpendicular to grain, respectively. The investigated spacing corresponded to the common requirement in European Technical Assessment documents (ETAs) for screws, given as $a_1 a_2 \geq 25 d^2$ and $a_2 \geq 2.5 d$. The nominal diameter of the self-tapping screws used was $d = 8$ mm.

4.2.4. Reference tests with single screws

For each different penetration length l_p and screw type used in these investigations reference, single screw withdrawal tests in the same material were made; these tests are further marked as “sgl”. All screws were tested in a “push-pull” setup according to EN 1382 [65]. Depending on the penetration length, steel tension and/or withdrawal failures were observed. The observed failure modes are subsequently considered in the statistical data analysis.

5. Results and discussion

5.1. Evaluation of failure mechanisms

To determine cracks in the cross section, after testing all specimens were cut through the middle of the group of screws. To assign each test to one of the failure mechanisms (block shear B1 or B2; see Fig. 3, withdrawal; see Fig. 18, steel, tension perpendicular to grain or splitting), the surface, the crack pattern and the corresponding load-displacement curve of each specimen were analysed. The splitting failure mechanism, as observed in series f'13, is characterized by cracks in-between rows of screws parallel to grain.

5.2. Definition of evaluated test loads

Some specimens which failed in block shear showed load-displacement curves with a load drop after an almost linear load increase. The maximum load up to this first significant partial failure is named F_{1st} .

The subsequent load-displacement curve featured a lower gradient, i.e. stiffness, as consequence of load redistribution within remaining load resisting (parts of) failure planes in tested groups of screws; see Fig. 22. In most cases the maximum load achieved within this second part of the load-displacement curve exceeded F_{1st} and is thus named as F_{max} . F_{1st} was evaluated only for load-displacement curves where the stiffness (tangential slip modulus) after the partial failure decreased by more than 10%; hereby the stiffness after the partial failure was determined within the load drop and the point exceeding F_{1st} .

5.3. Failure mechanisms and statistical evaluation of test series

The number (no.) of specimens which failed by block shear (B1 or B2), withdrawal, steel or other failure mechanisms are given Tables 5 and 6 in the Appendix. The data includes mean values X_i , mean and coefficients of variation CV for F_{1st} and F_{max} . In calculating the mean values of (sub)samples failing in block shear, both mechanisms, B1 and B2, are combined due to any obvious qualitative difference. In samples where a partial failure was not observed, an additional note is made in all tests.

5.4. Groups of screws: Withdrawal and steel failure mechanism

Within test setup T1, in some samples withdrawal failures also occurred; see Fig. 19. Either in tested free joints with $n = 4$ (s'10_A) and in restricted joints with $n = 9$ (s'10_E) or in groups featuring spacing $a_2 = 7 d$ (s'12_P, _Q & _R), only withdrawal or steel failures were observed. Back-calculating the withdrawal capacities of single screws by dividing the mean value of the maximum withdrawal load from group testing by the number of screws tested, i.e. $F_{W,max,mean}/n$, gives values slightly below the mean values of single screws failing in withdrawal, i.e. $F_{ax,sgl,mean}$. One reason therefore is seen in the right-censored withdrawal data in samples featuring withdrawal as well as steel failures, i.e. the withdrawal capacity in tests failing in steel can be assumed to be higher, but limited by the steel capacity. Thus, the withdrawal capacities for samples s'12_P, _Q & _R and corresponding test results with single screws (s'12_sgl) are estimated by means of the Maximum-Likelihood-Method for right-censored data; these values are further denominated as $F_{W,max,MLE}$, Table 5 in the Appendix. In Fig. 19 the 95% confidence interval CI_{95} for mean values of single withdrawal tests is also included. Its calculation is based on assumed lognormal distribution and done with the modified COX-Method; see Zhou and Gao [67] and Olsson [68].

In both test setups and samples featuring $a_2 > 2.5 d$, steel failures were observed. Back-calculating the steel capacities of single screws by dividing the mean values of maximum steel capacity from group testing by the number of screws tested, i.e. $F_{S,max,mean}/n$, gives values comparable to average steel capacities $F_{t,sgl,mean}$ gained from testing single screws, see Fig. 19 and Table 3. In samples s'12_P, _Q & _R only parts of

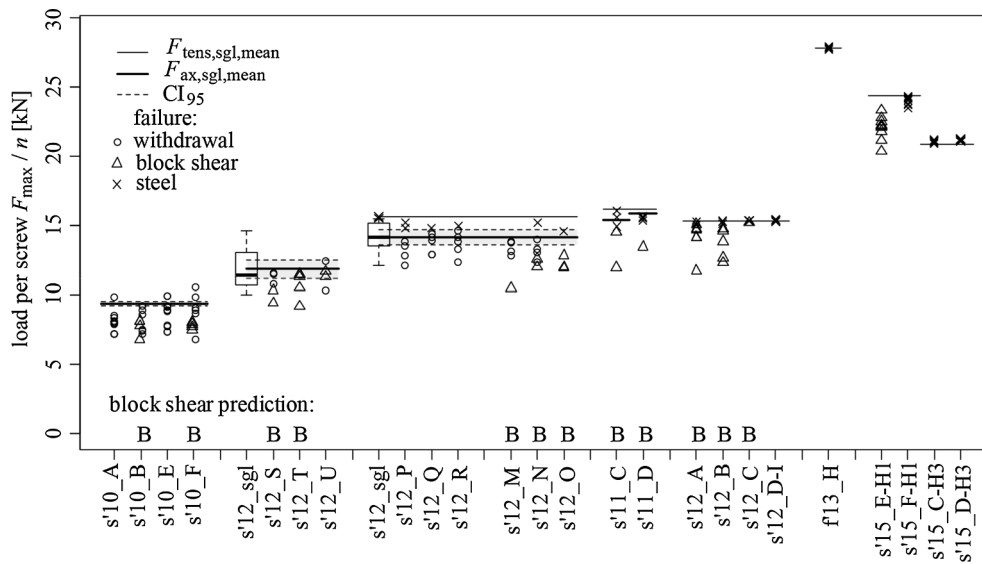


Fig. 19. Results of tests featuring mainly withdrawal or steel failures.

screws in tested groups failed in steel, see Table 5 in the Appendix. In view of the heterogeneity of timber, unequal load distribution between the screws is assumed and seen as a reason for $n_{ef,S} \geq 0.95$.

For groups of screws featuring only withdrawal failures, based on mean values the effective number of screws $n_{ef,W}$ was calculated with $n_{ef,W} = 0.86$ for small groups with $n = 4$ (s'10_A) and $n_{ef,W} \geq 0.92$ for all larger groups (s'10_E, s'12_P, _Q & _R), see Table 3. For samples also featuring some block shear failures, as s'10_B and s'10_F, similar values for n_{ef} are assumed.

By investigating spacing for groups of axially-loaded screws with the aim to maintain the characteristic withdrawal capacity of single screws times the number of screws in the group ($n_{ef} = n$), the spacing $a_1 \geq 7 d$ and $a_2 \geq (2.5-3.5) d$ have been found; see e.g. Blaß and Uibel [69] and Pluess and Brandner [70] for the narrow-face of CLT and Blaß et al. [9] for solid timber. It should be noted that these investigations are based on small groups or groups with only $s \leq 2$ columns.

5.5. Block shear failure model: Specific parameter settings

To be able to compare and validate the outcomes from the block shear model with experimental investigations, settings of model and material parameters, discussed more generally in Section 3, are specified according to the applied material and test setups. Observations made during testing, in particular regarding parameter settings leading to changing failure mechanisms, serve as a first decision basis for determining the length X_r and X_s . The consequence of losing some degree of independency between test results and model outcomes is thereby accepted.

Table 3

Effective number of screws n_{ef} of samples featuring mainly withdrawal or steel failures (basis: mean values).

Series	s'10				s'12			s'11		s'12				f'13	s'15		
Sample	A	B	E	F	P	Q	R	C	D	A	B	C	D-I	H	F-H1	C-H3	D-H3
$(l_{emb} + l_{ef})/d$	2 + 11.3				17.8			25.7		28.3				31.2	24.8		
n	4	9	9	16	12			16		12				10	9		
$n_{ef,W}$	0.86	0.87	0.92	0.96	-	-	-	-	-	-	-	-	-	-	-	-	-
$n_{ef,W,MLE}$	-	-	-	-	0.97	0.96	0.97	-	-	-	-	-	-	-	-	-	-
$n_{ef,S}$	-	-	-	-	0.96	0.95	0.96	0.96	0.96	0.99	1.00	1.00	1.00	0.99	0.98	1.01	1.02

Table 4

Settings of stress shape and load distribution parameters.

Model parameters	Test setup	Settings (min mean max)
$C_{t,90}$ [-]	T1 and T2	0.3 0.5 -
C_t [-]	T1 and T2	- 1.0 -
$C_s = C_r$ [-]	T1 and T2	0.8 0.9 1.0 0.9 1.0 -
X_r	T1 and T2	$2.0 d \left \min \left\{ 0.5(l_{top} - l_{group})_{perp. \ to \ grain} \right\} \right 2.8 d$ $2.5 d 5 d 7.5 d$
X_s	T1 and T2	$3.5 d 5 d 6.5 d$ $40 \text{ mm} 50 \text{ mm} 60 \text{ mm}$
$X_r = X_s$ restricted joints	T1	0.5 d

Mean material parameters and limiting values are defined in Section 3.2. Parameters $C_{t,90}$, C_t , C_r and C_s are determined according to Section 3.3, which are adapted according to the specific support conditions applied in the tests and outlined in Table 4.

In determining the length X_r of adjacent volume additionally active in rolling shear, observations from samples failing in block shear mechanism B1, requiring stress interaction from neighbouring screws, are taken into account. Samples tested by means of setup T1, featuring near circumferential or longitudinal support, indicate $0.5 (3.5 d) = 1.75 d \leq X_r \leq 0.5 (5 d) = 2.5 d$. The upper limit is argued as parts of samples

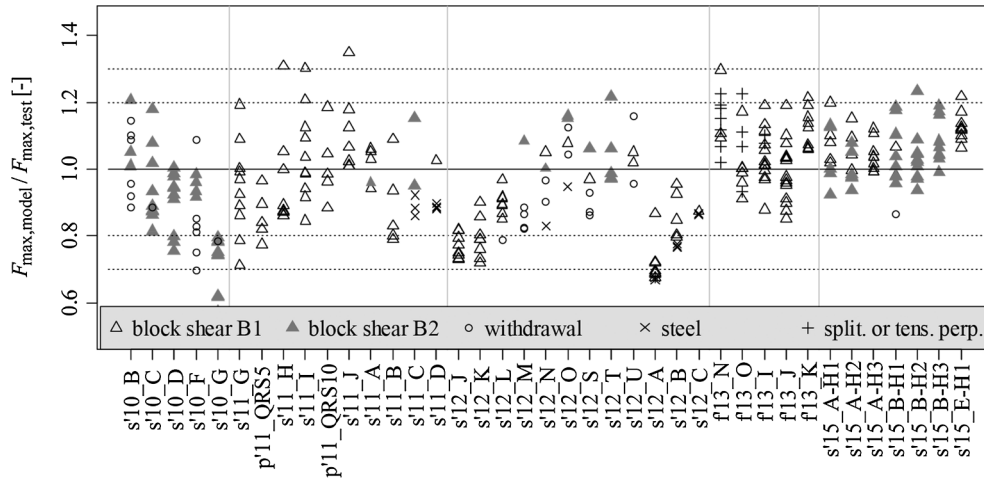


Fig. 20. Model predictions vs. test outcomes (mean values): validation with samples featuring (partial) block shear failures; apart from samples s'12_U and s'15_E block shear failure was predicted.

with spacing $a_2 = 5 d$ which featured either block shear B2 or withdrawal failures. For $l_{ef} < 20 d$ and $l_{ef} > 20 d$, analogue use of the load dispersion model of Van der Put [62], see Eq. (10), gives $X_r = 1.1 d$ to $2.1 d$ and $2.0 d$ to $2.8 d$, respectively. Finally, $X_r = 2.5 d$ was applied for validating samples from test setup T1, with $2 d$ and $2.8 d$ as lower and upper limits, respectively. For cases of tested restricted joints (s'10_E, _F & _G), $X_r = 0.5 d = 3 \text{ mm}$ was applied. Based on observations made from test setup T2, featuring significant additional bending stresses, $X_r \geq 0.5 (10 d) = 5 d$ can be concluded. $X_r = 2.5 d$ according to the approach of Van der Put [62], see Eq. (10), serves as a lower limit. In absence of a better estimate for the upper limit a symmetric bandwidth is chosen, given $X_r = 7.5 d$ as an upper limit.

In determining X_s for setup T1 again test outcomes, i.e. changing failure mechanism within the same sample, are taken into account. For example regarding pure block shear mechanism B1, for $a_2 = 3.5 d$ in sample s'12, at $a_1 = 10 d$ there was one withdrawal failure supporting $X_s \leq 5 d$. Same spacing a_2 in samples s'11_G to _J and p'11_QRS5 & _QRS10 with $a_1 = 5 d$ to $12.5 d$ indicate a slight higher value for X_s . On the other hand the observed combined block shear failure mechanism

B2 in series s'15 with settings $a_2 = 5 d$ and $a_1 = 7 d$ indicate $X_s \leq 3.5 d$. In conclusion, for test setup T1 featuring circumferential and longitudinal support conditions $X_s = 5 d \pm 1.5 d$ applies.

In samples tested according to setup T2 only a few variations in settings were investigated, thus possibilities for inferring settings for X_s from experiments are limited. In setup T2 the ratio of specimen height to distance between loading and support is about $H/(0.5 l_{op}) \sim 1:1$ and $1:1.5$, with loading and support at the same side of the beam. In contrast, the mechanical analogies discussed in Section 3.3.4 consider loading opposite to support; see Madsen et al. [57] and Tanahashi et al. [58], or are based on a theoretically infinite beam; see Barber [60], and Van der Put [62].

By means of the mechanical analogies as discussed in Section 3.3.4, the following values are found: applying Madsen et al. [57] and Tanahashi et al. [58], $X_s = 48\text{--}59 \text{ mm}$, which is only suitable for small values of $H - l_p$ (see f'13_O, _I & _J). The iterative approach of Barber [60], with stiffness according to Eq. (8), provides $X_s = 81$ and 89 mm for f'13_N & _K and f'13_O, _I & _J, respectively. By FEA of the length of the bottom plane stressed in tension perpendicular to the grain, for

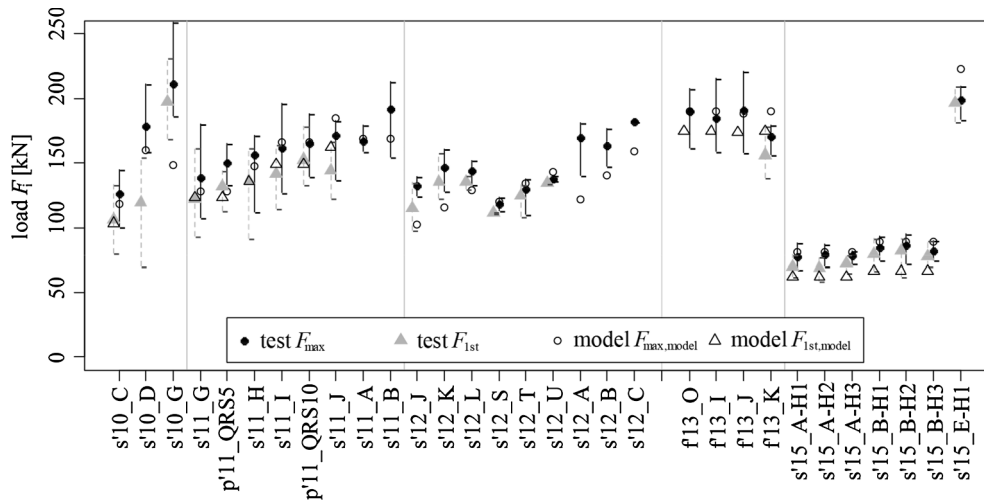


Fig. 21. Mean values of first failure and maximum capacities observed in tests and mean values of model predictions: comparison with samples featuring (partial) block shear failures.

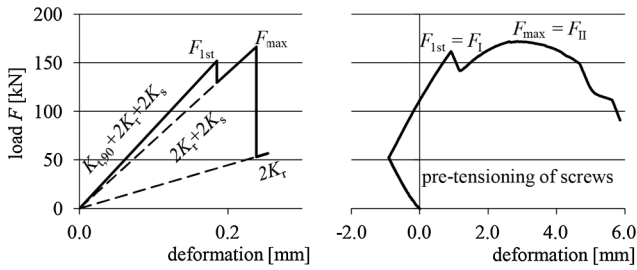


Fig. 22. Load-displacement response exemplarily for one axially-loaded group of screws: (left) response from block shear model; (right) response from a representative experimental investigation.

f'13_N & K X_s = 120 mm and for f'13_O, _I & _J X_s = 45 mm are determined. The approach of Van der Put [62] with X_s = 52 mm, see Eq. (10), gives more suitable values for the load spreading. Comparing sample f'13_N with f'13_K, by increasing a₁ from 5.3 d to 10.5 d (together with decreasing n from 10 to 8) block shear failure, as a main failure mechanism, could be avoided. Hence, it can be concluded X_s ≤ 0.5 (10.5 d), which would result in 42 mm, given d = 8 mm. To conclude, for test setup T2 X_s = 50 mm ± 10 mm as mean and limiting values are further applied.

5.6. Block shear model: Validation

5.6.1. Prediction of failure mechanism

Neither for steel nor for withdrawal failure mechanism n F_{sgl,mean} match the observed resistance of the group F_{group,mean}. However, for limitation of the withdrawal and steel capacity in the block shear model the corresponding resistance level n F_{sgl,mean} was taken. In case of groups featuring an l_p which would allow both failure mechanisms, the minimum value of withdrawal and steel resistance, min[n F_{w,sgl,mean,MLE}; n F_{s,sgl,mean}] is applied. In Fig. 19 the samples with model

prediction n F_{sgl,mean} > F_{max,model} are marked with “B” for block shear. In samples s'12_O, s'12_U and s'15_E-H1 failing partly in block shear, the ratio F_{max,model}/n F_{sgl,mean} meet 96%, 100% and 102%, respectively, constituting a good agreement between the model and the observed failure mechanisms. Fig. 19 additionally points out the reduced group resistance in case of block shear mechanism faced with withdrawal or steel failure mechanism in the same sample.

5.6.2. Comparison of resistances

Figs. 20 and 21 visualize a comparison between mean block shear model and mean test outcomes on a relative and absolute basis of samples failing completely or partly in block shear. In Fig. 20 overall a good representation of test data by the model can be observed with ratios F_{max,model}/F_{max,test,mean} varying within ± 20%. The predictions are found to agree well with both block shear failure mechanisms, B1 and B2. As expected, in samples also featuring other failure mechanisms together with a block shear B2 crack pattern values slightly above the predictions were determined in testing. The reason is the transition to other failure mechanisms, which in its current state is not represented by the block shear model. For example in sample f'13_N row shear and tension perpendicular to grain failure mechanisms dominated. The reason for this is seen in the low ratio l_p/H = 52%. The model prediction slightly overestimates this sample. For samples s'12_A, _B & _C, featuring very small spacing due to the penetration depth capacities rather close to steel failure mechanism. For samples with restricted joints, s'10_F & _G, a decreasing accuracy in model predictions with increasing n is found.

Apart from the maximum capacity, also for the first failure good and acceptable agreement between model predictions and test outcomes (mean values) is given, except for sample s'10_D with F_{1st} > 0.84 F_{max}; see Fig. 21. The model also predicted no first failure for samples of series s'11, although first failures were observed. On the contrary, in series f'13 the model predicts first failures, but none were observed. Overall, the model and test outcomes are rather close.

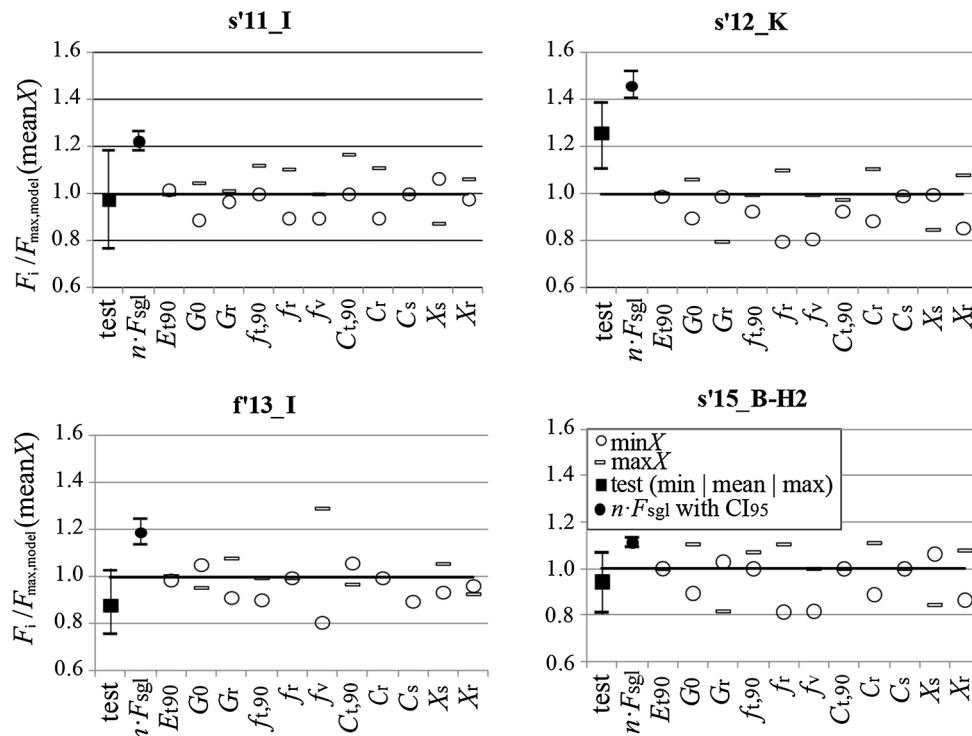


Fig. 23. Sensitivity study on block shear model parameters exemplarily for some selected test samples.

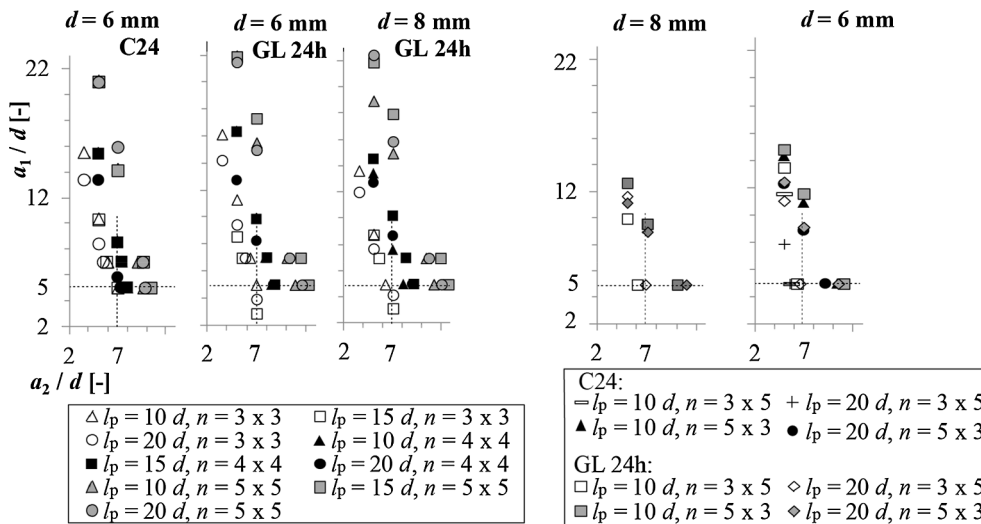


Fig. 24. Parameter study for groups with $n = r \times s$ screws featuring either a nominal diameter of $d = 6$ or 8 mm, inserted either in GL 24 h according to EN 14080 [19] or C24 according to EN 338 [18] with adapted geometric parameters, i.e. penetration length l_p and spacing a_1 and a_2 , to fail in withdrawal prior to block shear failure by fulfilling the condition $F_{\text{model}}/(n F_{\text{ax,mean}}) \geq 1.05$.

5.6.3. Stiffness

The absolute model stiffness, see Fig. 22 (left), is significantly higher than the stiffness observed from corresponding experimental load-displacement curves, see Fig. 22 (right). These significant deviations can be explained by the applied displacement-measurement in testing groups of screws. Thereby determined displacements comprise the elongation of the partially long screw shanks, the compression of the timber surface at the supports as well as the displacement of the screw group in timber as some kind of a composite stiffness of steel thread interacting with timber. Furthermore, within the block shear model ideal linear elastic material response is assumed. In reality the timber as well as the steel itself feature a significant amount of non-linear, elastic-plastic behaviour.

5.6.4. Sensitivity study on block shear model parameters

For exemplarily analysing the sensitivity of all parameters in the block shear model, four test samples are chosen with mainly block shear failures: s'11_I and s'12_K of test setup T1 with circumferential support and $F_{\text{max,test,mean}}/F_{\text{max,model}} \cong 1.0$ and 1.25 , respectively, s'15_B-H2 with support only in transverse direction and f'13_I of test setup T2. The sensitivity is tested by setting the limit values (minimum and maximum) instead of the mean values for the model parameter of interest, while for all other model parameters their mean values are applied. In doing so, effects from changed settings in more than one parameter are not considered. In addition, minimum and maximum of $F_{\text{max,test,min}}/F_{\text{max,model}}$ and $F_{\text{max,test,max}}/F_{\text{max,model}}$, as well as $n F_{\text{sgl,mean}}/F_{\text{max,model}}$ applying the upper and lower values of the 95% confidence interval CI_{95} calculated for the single withdrawals tests are given, see Fig. 23.

The modulus of elasticity in tension perpendicular to grain, $E_{t,90}$, and the stress shape parameter $C_{t,90}$ influence the maximum capacity estimated by the model only marginally, i.e. variation is only $\pm 14\%$. This is because the share of load transmitted via the bottom plane $A_{t,90}$ is small and in most cases becomes zero at the first failure. Although the limits in shear and rolling shear modulus, G_0 and G_r , respectively, correspond to a variation of ± 20 to 40% , their influence on the capacities is also found to be small. The same is also observed for the stress shape parameters $C_{t,90}$, C_r and C_s , however, their limit values vary no more than $\pm 10\%$. In contrast, the material parameters f_t and f_v as well as the stress shape parameters X_r and X_s are identified as the main influencing parameters for the model outcomes.

5.7. Study on geometric parameters to assure withdrawal failure

In the following, the block shear model is used to predict the

required geometric arrangement, i.e. spacing a_1 and a_2 and penetration length l_p , of the axially-loaded group of screws preconditioning withdrawal instead of block shear failure. For the material parameters settings for GL 24 h according to EN 14080 [19] and C24 according to EN 338 [18] are applied, see Table 1. Settings for the stress shape parameters as well as for loading and supporting conditions, mirroring test setup T1 with circumferential support, are taken from Table 4. Consequently, the opening length L_{op} and width W_{op} is adopted with $(r + 1) a_1$ and $(s + 1) a_2$, respectively, which becomes relevant only in calculation for distances of external screws to support shorter than $5 d$ and $2.5 d$, respectively, see Table 4. The analysis focuses on screws featuring a nominal diameter of $d = 6$ or 8 mm and a penetration length $l_p = 10 d$, $15 d$ and $20 d$. The withdrawal resistance of single screws, $F_{\text{ax,mean}}$ is calculated according to the approach in Ringhofer et al. [71] and Ringhofer [2]. For $l_p = 20 d$, which already demarks the border to steel failure of screws, and diameter $d = 6$ and 8 mm withdrawal capacities of $F_{\text{ax,mean}} = 14.3$ kN and 23.1 kN, respectively, are given. For groups of $n = r \times s$ screws with $n_{\text{max}} = 25$ either spacing $a_1 = 5 d$ | $7 d$ or $a_2 = 3.5 d$ | $5 d$ | $7 d$ is fixed and a_2 or a_1 , respectively, adapted to fulfil the condition $F_{\text{model}}/(n F_{\text{ax,mean}}) \geq 1.05$. The factor 1.05 is derived from test series and marks the upper limiting value where block shear and withdrawal or rather steel failure could be observed.

Fig. 24 shows that for both nominal strength classes, glulam GL 24 h according to EN 14080 [19] and solid timber C24 according to EN 338 [18], for both nominal diameters $d = 6$ and 8 mm as well as for penetration lengths $l_p = 10 d$ up to $20 d$ withdrawal is the leading failure mechanism as long as spacing $a_1 = 5 d$ and $a_2 = 7 d$ and the number of screws in a row in grain is $r \leq 3$. The relevance of r is particularly apparent when comparing the outcomes for $n = 5 \times 3$ and $n = 3 \times 5$.

The outcomes of the geometric parameter study are in accordance with the test results of samples which failed in withdrawal (s'12_P, _Q, _R, s'10_A and _E). It should be noted that samples with $a_2 = 7 d$ are tested only with $r \leq 3$.

One conclusion from the parameter study is that the penetration length l_p proves to have only a minor influence whereas adequate settings for the geometric parameters a_1 and a_2 together with parameter r are mandatory, even for groups of screws featuring penetration lengths provoking steel failure. However, samples of test series which failed completely in steel confirm common regulations in ETAs with $a_1 a_2 \geq 25 d^2$. Penetration lengths of screws in samples s'12_C to _I, f'13_H, s'15_C, _D and _F are relatively high; $l_p \geq 28 d$ which is due to a higher steel capacity of screws used in those groups. Based on the current state of knowledge, for groups of screws prone to failing in steel, the current regulation $a_1 a_2 \geq 25 d^2$ can be applied as long as the following requirements are fulfilled: $a_1 \geq 5 d$, $a_2 \geq 3.5 d$ and $F_{\text{model}} > (1.05 n F_t)$.

6. Summary, conclusions & outlook

This paper focused on the block shear mechanism as a rather brittle group failure mechanism which has been recently reported for the first time and still lacks regulation. This failure mechanism is defined as failure of the planes surrounding the group of screws. These planes are exposed either to shear, rolling shear or tension perpendicular to grain stresses.

In a comprehensive experimental campaign over 300 tests on axially-loaded groups of screws were made by means of two different and especially developed test setups. The main series with screw groups inserted at an angle of 90° between the screw axis and the grain were presented and the resistance and failure mechanisms are analysed. Apart from withdrawal and steel failures, mainly block shear failures were observed even at design of groups of screws, i.e. $a_1 a_2 \geq 25 d^2$, which are currently allowed in EC 5 [3] and ETAs, but with capacities partly significantly lower than predicted based on current regulations. Block shear failures comprising tension perpendicular to grain failure were also observed at $l_{ef}/H_{beam} > 0.7$, a ratio that is currently recommended to prevent failures in tension perpendicular to grain. It occurred also in a variety of “push-pull” setups featuring distant or near supports as well as in configurations featuring free and restricted surface deformations.

The mechanically based, deterministic block shear failure model for a screw group with a thread-fibre angle of $\alpha = 90^\circ$ proposed by Mahlkecht et al. [7] and [8] identifies this three-dimensional failure mechanism as resistance of three parallel acting (failure) planes or rather plane pairs. Load sharing and load redistribution after partial failure(s) are thereby defined by the individual stiffness of all planes still active in load bearing. The 19 model parameters for characterising the geometry, material properties and stress distribution are thoroughly analysed and adapted for each test setup to compare the model with test results. The geometry parameters, e.g. spacing, penetration length and group size, are fixed by the group design, its geometric arrangement or layout. For the material parameters, the elastic properties $E_{t,90}$, G_0 & G_r and the strength properties $f_{t,90}$, f_v & f_r are implemented as mean values based on data from literature and our own investigations, for both investigated nominal strength classes, GL 24 h for glulam according to EN 14080 [19] and C24 for solid timber according to EN 338 [18]. For determination of the stress shape parameters, the analysis of test results, also with respect to observed failure mechanisms versus screw arrangement, investigations via a two-dimensional FE model and similar mechanical models were made. The stress shape parameters were hence adapted to the specific load and support conditions of the test setups; i.e. for near (circumferential) support conditions equal to the first test setup T1 and for distant support conditions equal to the single span girder test setup T2, additionally featuring a relevant amount of bending stresses. For most of the tested samples featuring block shear failures a good agreement with the block shear failure model, i.e. the capacities at first partial failure and the maximum capacities, was observed. Including the withdrawal and steel failure mechanism with $n F_{ax,sgl}$ and $n F_{t,sgl}$, respectively, allows to predict the leading failure mechanism out of these three failure mechanisms. Apart from that, further inclusion of a potential failure in the net cross section can be easily achieved, but was not done so far. Considering uncertainty caused by the assumptions made for deriving this block shear failure model, i.e. $n_{ef} = n$, it can be observed that within a range of $1.00 \pm 0.05 n F_{sgl,mean}/F_{max,model}$ each of these failure mechanism, i.e. block shear, withdrawal, steel or net cross section failure mechanism, or combinations of them can occur; see also Figs. 19 and 20. To ensure

that a block shear failure can be safely prevented, i.e. that other failures happen prior to block shear failure, it is suggested to keep $n F_{sgl,mean} > 1.05 F_{max,model}$.

Requirements on the geometry of groups of screws aiming at withdrawal failure or failure in the net cross section instead of block shear failure are found by considering test outcomes and by means of a parameter study with the block shear model. In this parameter study and for specific settings of penetration depth l_p and group size $n = r \times s$ the spacing a_1 and a_2 were adapted to achieve withdrawal prior to block shear failure. For C24, according to EN 338 [18] and GL 24 h according to EN 14080 [19], loading and supporting conditions according to test setup T1, screw diameters $d = 6$ mm and 8 mm and based on mean values, the following recommendations can be made: spacing in grain $a_1 \geq 5 d$, spacing perpendicular to grain $a_2 \geq 7 d$ and additionally the number of rows of screws in the group $r \leq 3$. Hereby the number of screws in series in grain, r , was found to influence the requested spacing decisively.

For the investigated material, group arrangement and loading and supporting conditions, for groups failing in steel the current requirement $a_1 a_2 \geq 25 d^2$ anchored in diverse ETAs can be confirmed as long as $a_1 \geq 5 d$, $a_2 \geq 3.5 d$ and $F_{model} > (1.05 n F_t)$.

With respect to the accountable number of commonly acting screws in a group and observed failure modes, on the basis of mean values for withdrawal and steel resistance, the test outcomes show $0.90 n F_{ax,sgl}$ for groups failing in withdrawal and $0.95 n F_{t,sgl}$ for groups failing in steel. The reduction is related to unequal loading as a consequence of material heterogeneity, imperfect torque moment, unequal loading as a consequence of widely constraint equal deformation of external and internal screws in both analysed test setups and differences in the stress distribution along the penetration length of internal and external screws, which has an even higher impact on n_{ef} in groups of only a few screws, e.g. $n_{ef} = 0.85 n$ in sample s'10_A featuring $n = 4$ screws. The outcome agrees well with investigations by means of the probabilistic model proposed by Brandner et al. [56]. Although for the 5%-quantile, where even higher n_{ef}/n values are expected, which is due to the reduced variability (homogenisation) in comparison to single screw properties, for inclined screws comparable findings are given and suggestions made in Krenn [10] and Krenn and Schickhofer [11], with $0.9 n F_{t,sgl}$.

As a next step, it is intended to extend the successfully validated mechanically-based block shear model to a probabilistic block shear model by inclusion of uncertainties of input parameters and their possible correlations as well as model uncertainties. Furthermore, the brief sensitivity study on model parameters has to be extended to investigate also the interaction of a set of parameters instead of changing the setting only for one parameter each. To ease its practicality, it is aimed to simplify the block shear model as far as reasonably practicable and thus to provide a verification procedure for design standards. In this respect, it is also envisaged to come up with a suitable test setup for determining minimum spacing and end- and edge-distances applicable for diverse failure mechanisms.

Acknowledgements

The research work within the FFG BRIDGE-project “SCREWS” at the Institute of Timber Engineering and Wood Technology of the University of Graz and within the FFG COMET K-project “focus_sts” at the holz.bau forschungsbau gmbh is financed by Austrian Funding Agency FFG and by contributions of local governments as well as economical and scientific project partners. Their support is thankfully acknowledged.

Appendix A

See Tables 5 and 6.

Table 5
Parameters & results of series s'10, s'11, p'11, s'12 & s'15.

Main parameters & settings			Specimen geometry									
Series_sample [-]	No. of tests [-]	Arrangement	$l_{emb}/d_{le}/d$ [-]	$r s n$ [-]	$\alpha_1/d a_2/d$ [-]	H_{sp} [mm]	H_{cs} [mm]	W_{sp} [mm]	W_{cs} [mm]	l_{sp} [mm]		
s'10_A	10	2 11.3	2 2 4	5 5	-	113	-	-	175	370		
_B	10	2 11.3	3 3 9	5 5	286	113	370	370	175	370		
_C	10	2 11.3	4 4 16	5 5	286	113	370	370	175	370		
_D	10	2 11.3	5 5 25	5 5	286	113	370	370	175	370		
_E	11	2 11.3	3 3 9	5 5	-	113	-	-	175	370		
_F	10	2 11.3	4 4 16	5 5	286	113	370	370	175	370		
_G	10	2 11.3	5 5 25	5 5	286	113	370	370	175	370		
_sgl	128	2 11.3	1	-	-	113	-	-	175	180		
s'11_A	5	0 25.7	4 4 16	5 3.5	252	163	320	320	256	336		
_B	5	0 25.7	4 4 16	5 3.5	-	163	-	-	256	400		
_C	5	0 25.7	4 4 16	5 5	252	163	320	320	256	336		
_D	5	0 25.7	4 4 16	5 5	-	163	-	-	256	400		
_sgl	20	0 25.7	1	-	252	163	320	320	256	336		
_sgl	20	0 25.7	1	-	-	163	-	-	256	400		
_G	10	4 11.3	5 5 25	5 3.5	252	163	320	320	256	370		
_H	9	4 11.3	5 5 25	7.5 3.5	252	163	320	320	256	400		
_I	10	4 11.3	5 5 25	10 3.5	252	163	320	320	256	460		
_J	9	4 11.3	5 5 25	12.5 3.5	252	163	320	320	256	530		
_sgl	10	4 11.3	1	-	252	163	320	320	256	460		
_sgl	57	2 11.3	1	-	-	163	-	-	256	180		
s'12_A	10	0 28.3	3 4 12	5 2.5	240	240	340	340	180	350		
_B	9	0 28.3	3 4 12	7.5 2.5	240	240	340	340	180	350		
_C	5	0 28.3	3 4 12	10 2.5	240	240	340	340	180	350		
_D	5	0 28.3	3 4 12	5 3.5	240	240	340	340	180	350		
_E	2	0 28.3	3 4 12	7.5 3.5	240	240	340	340	180	350		
_F	2	0 28.3	3 4 12	10 3.5	240	240	340	340	180	350		
_G	5	0 28.3	3 4 12	5 5	240	240	340	340	180	350		
_H	2	0 28.3	3 4 12	7.5 5	240	240	340	340	180	350		
_I	5	0 28.3	3 4 12	10 5	240	240	340	340	180	350		
_J	8	0 17.8	3 4 12	5 3.5	240	240	340	340	180	350		
_K	8	0 17.8	3 4 12	7.5 3.5	240	240	340	340	180	350		
_L	8	0 17.8	3 4 12	10 3.5	240	240	340	340	180	350		
_M	5	0 17.8	3 4 12	5 5	240	240	340	340	180	350		
_N	5	0 17.8	3 4 12	7.5 5	240	240	340	340	180	350		
_O	6	0 17.8	3 4 12	10 5	240	240	340	340	180	350		
_P	6	0 17.8	3 4 12	5 7	240	240	340	340	180	350		
_Q	6	0 17.8	3 4 12	7.5 7	240	240	340	340	180	350		
_R	6	0 17.8	3 4 12	10 7	240	240	340	340	180	350		
_S	5	0 14.2	3 4 12	5 5	240	240	340	340	180	350		
_T	5	0 14.2	3 4 12	7.5 5	240	240	340	340	180	350		
_U	4	0 14.2	3 4 12	10 5	240	240	340	340	180	350		
_sgl	20	0 17.8	1	-	-	240	-	-	180	180		
_sgl	20	0 14.2	1	-	-	240	-	-	180	180		
_sgl	39	0 28.3	1	-	-	-	-	-	-	-		
s'15_A-HI	10	0 8.8	3 3 9	5 5	-	160	-	-	190	600		
A-H2	10	0 8.8	3 3 9	5 5	-	160	-	-	190	600		
_A-H3	10	0 8.8	3 3 9	5 5	-	160	-	-	190	600		
_B-H1	10	0 8.8	3 3 9	7 5	-	160	-	-	190	600		

(continued on next page)

Table 5 (continued)

Main parameters & settings				Specimen geometry											
Series_sample [-]	No. of tests [-]	Arrangement		$l_{comb}/d l_{ker}/d$ [-]	$r s n$ [-]	$\alpha_1/d \alpha_2/d$ [-]	H_{sp} [mm]	H_{cs} [mm]	W_{sp} [mm]	W_{cs} [mm]	l_{sp} [mm]				
_B-H2	10	0 8.8		0 8.8	3 3 9	7 5	-	160	-	190	600				
_B-H3	10	0 8.8		0 8.8	3 3 9	7 5	-	160	-	190	600				
_C-H3	10	0 24.8		0 24.8	3 3 9	5 5	-	280	-	190	600				
_D-H3	5	0 24.8		0 24.8	3 3 9	7 5	-	280	-	190	600				
_E-H1	10	0 24.8		0 24.8	3 3 9	5 5	-	280	-	190	600				
_F-H1	10	0 24.8		0 24.8	3 3 9	7 5	-	280	-	190	600				
_sgl	16	0 8.8		0 8.8	1	-	-	160	-	185	175				
_sgl	18	0 8.8		0 8.8	1	-	-	160	-	185	175				
_sgl	20	0 8.8		0 8.8	1	-	-	160	-	185	175				
_sgl	10	0 23.8		0 23.8	1	-	-	-	-	-	-				
_sgl	10	0 23.8		0 23.8	1	-	-	-	-	-	-				
p 11_QRS5	5	4 11.3		4 11.3	5 5 25	5 3.5	-	163	-	256	-				
_ORS10	5	4 11.3		4 11.3	5 5 25	10 3.5	-	163	-	256	-				

Main parameters & settings				Results				Withdrawal failure				Steel failure				Density all			
Series_sample [-]	Support geometry	l_{op} [mm]	W_{op} [mm]	No. type [-]	$F_{B,1st}$ mean [kN]	$F_{B,1st}$ CV [%]	$F_{B,max}$ mean [kN]	$F_{B,max}$ CV [%]	No. [-]	$F_{S,max}$ mean [kN]	$F_{S,max}$ CV [%]	ρ_{12} mean [kg/m ³]	mean [CV]	ρ_{12} mean [CV]	Comments [-]				
s 10_A		144	144	0	-	-	32.0 9.9	-	0	-	-	399 4.1	-	-	-				
B		144	144	4 B2	55.0 ^a	-	69.3 8.2	-	6	-	-	419 7.9	-	-	* F{1st} in 2/4 tests				
_C		144	144	9 B2	106 18.8	-	126 11.6	-	1	-	-	437 14.6	-	-	-				
_D		144	144	10 B2	119 24.2	-	179 10.8	-	0	-	-	452 9.0	-	-	-				
_E		0	0	0	-	-	-	-	11	-	-	428 10.5	-	-	-				
_F		0	0	4 B2	109 7.1	-	124 3.1	-	6	-	-	435 10.8	-	-	-				
G		0	0	7 B2	198 11.9	-	211 12.9	-	1	-	-	437 11.2	-	-	* F{1st} in 6/9 tests				
sgl		0	0	2 B1	-	-	-	-	128	-	-	446 10.3	-	-	* Cl{95} 9.12 9.51				
s 11_A		144	144	1 B2	-	-	167 5.5	-	0	-	-	403 7.7	-	-	-				
_B		144	144	4 B1	-	-	-	-	0	-	-	415 2.8	-	-	-				
_C		144	144	5 B1	-	-	192 12.7	-	0	-	-	395 10.7	-	-	-				
_D		144	144	2 B2	-	-	201 ^a	-	3	-	-	248 3.6	-	-	-				
_sgl		0	0	1 B1	-	-	215 ^a	-	4	-	-	248 0.8	-	-	-				
_sgl		0	0	0	-	-	-	-	9	-	-	407 3.4	-	-	ref_A, _C				
sgl		0	0	0	-	-	-	-	11	-	-	16.2 0.5	-	-	* $F{W,max,MLE}$ = -				
sgl		0	0	0	-	-	-	-	3	-	-	407 10.5	-	-	* $F{W,max,MLE}$ = -				
_G		180	126	10 B1	122 17.9	-	139 15.3	-	0	-	-	408 8.4	-	-	16.4 7.2				
_H		270	126	9 B1	136 17.7	-	157 12.8	-	0	-	-	401 9.7	-	-	ref_B, _D				
J		360	126	10 B1	141 13.3	-	162 13.0	-	0	-	-	408 8.4	-	-	* F{1st} in 9/10 tests				
J		450	126	9 B1	144 14.7	-	172 9.4	-	0	-	-	401 9.7	-	-	* F{1st} in 7/9 tests				
sgl		0	0	0	-	-	-	-	10	-	-	408 8.4	-	-	* F{1st} in 6/10 tests				
															* F_{1st} in 6/9 tests				
															$l_{comb} = 4$ d				

(continued on next page)

Table 5 (continued)

Main parameters & settings		Results										
Series_sample [-]	Support geometry		Block shear failure			Withdrawal failure			Steel failure		Density all	Comments [-]
	L_{op} [mm]	W_{op} [mm]	No. type [-]	$F_{B,1st}$ mean CV [kN] [%]	$F_{B,max}$ mean CV [kN] [%]	No. [-]	$F_{W,max}$ mean CV [kN] [%]	No. [-]	$F_{S,max}$ mean CV [kN] [%]	ρ_{12} mean CV [kg/m ³] [%]		
sgl	-	Ø 42	0	-	-	8.12 12.7*	0	-	-	403 8.8	$l{emb} = 2d$ *Cl ₉₅ 7.86–8.40	
s*12_A	120	75	7 B1	-	170 8.0	-	0	-	182	454 3.4	1 spec.: cracks along outer screw rows F = 181 kN	
_B	180	75	4 B1	-	164 8.1	-	0	-	183 0.5	453 3.1	-	
_C	240	75	1 B1	-	182 -	-	0	-	184 0.2	446 3.1	-	
_D	120	105	0	-	-	-	0	-	184 0.3	454 2.7	-	
_E	180	105	0	-	-	-	0	-	184 0.3	454 2.7	-	
_F	240	105	0	-	-	-	0	-	184 0.3	454 2.7	-	
_G	120	150	0	-	-	-	0	-	184 0.3	454 2.7	-	
_H	180	150	0	-	-	-	0	-	184 0.3	454 2.7	-	
_J	240	150	0	-	-	-	0	-	184 0.3	454 2.7	-	
_K	120	105	8 B1	115* 13.0	133 4.7	-	0	-	-	461 5.2	*F _{1,st} in 5/8 tests	
_L	180	105	8 B1	136* 11.5	146 7.5	-	0	-	-	446 2.6	*F _{1,st} in 4/8 tests	
_M	240	105	7 B1	136* 3.1	144 4.2	1	164 -	0	-	445 1.5	*F _{1,st} in 6/7 tests	
_N	120	150	1 B2	126 -	126 -	4	161 3.6	0	-	444 1.9	*all screws failed	
_O	180	150	2	134 -	147 -	2	162 -	1	182 -	460 2.5	*5/12 screws failed	
_P	240	150	3	135 -	147 -	2	153 -	1	175 -	452 2.3	*F _{W,maxMLE} 168 11.0	
_Q	120	210	0	-	-	-	4	157 6.0*	180* -	452 3.4	**9/12 and 11/12 screws failed	
_R	180	210	0	-	-	163 5.2*	5	163 5.2*	178* -	459 3.4	*F _{W,maxMLE} 166 6.2	
_S	240	210	0	-	-	164 6.3*	5	164 6.3*	180* -	458 4.0	**7/12 screws failed	
_T	120	150	2 B2	112 -	118 -	3	135 -	0	-	453 3.7	*F _{W,maxMLE} 167 7.3	
_U	180	150	5 B2	124 7.5	129 9.1	0	-	0	-	449 1.8	**11/12 screws failed	
_sgl	240	150	2 B2	134 -	138 -	2	136 -	0	-	466 4.4	-	
_sgl	-	Ø 42	0	-	-	14.1 7.2*	17	14.1 7.2*	15.6	449 7.2	*Cl ₉₅ 13.6–14.7	
s*15_A-HI	240	Ø 42	0	-	-	11.9 12.0*	20	11.9 12.0*	-	448 4.8	*F _{W,maxMLE} 14.4 8.5	
_sgl	-	-	0	-	-	-	0	-	15.3 0.6	-	*Cl ₉₅ 11.2–12.5	
s*15_A-HI	240	-	5 B1	70.1 8.6	77.1 7.8	0	-	0	-	402 3.5	-	

(continued on next page)

Table 5 (continued)

Main parameters & settings		Results											
Series_sample [-]	Support geometry		Block shear failure			Withdrawal failure			Steel failure		Density all		Comments [-]
	L_{op} [mm]	W_{op} [mm]	No. type [-]	$F_{B,1st}$ [kN] mean CV [%]	$F_{B,max}$ [kN] mean CV [%]	No. [-]	$F_{W,max}$ [kN] mean CV [%]	No. [-]	$F_{S,max}$ [kN] mean CV [%]	$\rho_{1,2}$ mean [kg/m ³] CV [%]			
_A-H2	240	-	4 B1 6 B2 10 B1	69.0 8.4	79.3 6.4	0	-	0	-	408 2.7			
A-H3	240	-	10 B1	72.5* 6.1	78.3 4.1	0	-	0	-	398 2.2		* $F{1,st}$ in 9/10 tests	
B-H1	240	-	2 B1 7 B2	79.7* 8.6	84.8 7.8	1	103	0	-	397 3.8		* $F{1,st}$ in 8/9 tests	
B-H2	240	-	10 B2	82.3* 10.3	86.4 7.3	0	-	0	-	408 2.7		* $F{1,st}$ in 9/10 tests	
B-H3	240	-	10 B2	77.7* 7.0	81.6 6.4	0	-	0	-	397 4.3		* $F{1,st}$ in 8/10 tests	
_C-H3	240	-	0	-	-	0	-	10	190 0.4	418 4.8			
_D-H3	240	-	0	-	-	0	-	5	191 0.4	420 4.6%			
E-H1	240	-	3 B1 7 B2	197* 3.8	199 3.7	0	-	0	-	400 2.2		* $F{1,st}$ in 3/10 tests	
_F-H1	240	-	0	-	-	0	-	10	216 1.1	415 2.3			
_sg1	-	Ø 56	0	-	-	16	10.8 15.9	0	-	413		H1	
_sg1	-	Ø 56	0	-	-	18	11.0 9.3*	0	-	410		H2	
_sg1	-	Ø 56	0	-	-	20	10.3 10.0	0	-	422		H3	
_sg1	-	-	0	-	-	0	-	10	24.4 1.7	-		H1	
_sg1	-	-	0	-	-	0	-	10	20.8 1.1	-		H3	
p711_QRS5	180	126	5 B1	132* 10.0	150 8.5	-	-	-	-	400 9.6		* $F_{1,st}$ in 4/5 tests	
_QRS10	360	126	5 B1	153 13.5	167 10.9	-	-	-	-	400 9.6		-	

References

- [1] Ringhofer A, Brandner R, Grabner M, Schickhofer G. Ausziehfestigkeit selbstbohrender Holzschrauben in geschichteten Holzprodukten. *Forschungskolloquium Holzbau*, Stuttgart (D) 2014:49–60.
- [2] Ringhofer A. Axially loaded self-tapping screws in solid timber and laminated timber products. Doctoral Thesis. Graz University of Technology (A); 2017.
- [3] EN 1995-1-1:2014-05 Eurocode 5: Design of timber structures – Part 1-1: General – Common rules and rules for buildings. CEN.
- [4] Pleschounig S. Ausziehverhalten axial beanspruchter Schraubengruppen. Master Thesis. Graz University of Technology (A); 2010.
- [5] Mahlknecht U. Untersuchung von rechtwinklig zur Faser eingebrachten, axial beanspruchten Schraubengruppen im Vollholz und Brettspertholz. Master Thesis. Graz University of Technology (A); 2011.
- [6] Mahlknecht U, Brandner R. Untersuchungen des mechanischen Verhaltens von Schrauben – Verbindungsmittelgruppen in VH, BSH und BSP – Forschungsbericht. holz.bau forschungsbw gmbh –. Graz: University of Technology (A); 2013.
- [7] Mahlknecht U, Ringhofer A, Brandner R, Schickhofer G. Resistance and failure modes of axially loaded groups of screws. *Materials and joints in timber structures*, RILEM Bookseries 2014;9:289–300.
- [8] Mahlknecht U, Brandner R, Augustin M. Block shear failure mode of axially loaded groups of screws. *Proceeding of the WCTE*, Vienna (A); 2016.
- [9] Blaß HJ, Bejtka I, Uibel T. Tragfähigkeit von Verbindungen mit selbstbohrenden Holzschrauben mit Vollgewinde. *Karlsruher Berichte zum Ingenieurholzbau 4*. Universitätsverlag Karlsruhe (D); 2006.
- [10] Krenn H. Ein Beitrag zur Stahlblech-Holz-Zuglaschenverbindung mit geneigt angeordneten selbstbohrenden Holzschrauben. Dissertation, Graz University of Technology (A); 2017.
- [11] Krenn H, Schickhofer G. Joints with inclined screws and steel plates as outer members. *Proceeding of 42th CIB-W18-meeting*, Duebendorf (CH); 2009.
- [12] Foschi RO, Longworth J. Analysis and design of giplam nailed connections. *J Struct Div-ASCE* 1975;101(12):2537–55.
- [13] Kangas J, Vesa J. Design on timber capacity in nailed steel-to-timber joints. *Proceeding of 31th CIB-W18-meeting*, Savonlinna (Finland); 1998.
- [14] Stahl DC, Wolfe RW, Begel M. Improved analysis of timber rivet connections. *J Struct Eng* 2004;130(8):1272–9.
- [15] Zamani P, Quenneville P. Predictive analytical model for wood capacity of rivet connections in glulam and LVL. *Proceeding of 45th-CIB-W18-meeting*, Växjö (S); 2012.
- [16] Jöbstl RA, Bogensperger T, Schickhofer G. In-plane shear strength of Cross Laminated Timber. *Proceeding of 41th CIB-W18-meeting*, St. Andrews (Canada); 2008.
- [17] Brandner R, Dietsch P, Dröscher J, Schulte-Wrede M, Kreuzinger H, Sieder M. Cross laminated timber (CLT) diaphragms under shear: test configuration, properties and design. *Constr Build Mater* 2017;147:312–27.
- [18] EN 338:2003-07 Structural timber – Strength classes. CEN.
- [19] EN 14080:2013-06 Timber structures – Glued laminated timber and glued solid timber – Requirements. CEN.
- [20] Blaß HJ, Ehlbeck J, Schmid M. Ermittlung der Querkzugfestigkeit von Voll- und Brettschichtholz. *Forschungsbericht: University of Karlsruhe (D)*; 1998.
- [21] Mahlknecht U, Brandner R. Untersuchungen des mechanischen Verhaltens von Schrauben – Verbindungsmittelgruppen in VH, BSH und BSP – Ergänzung – Forschungsbericht. holz.bau forschungsbw gmbh –. Graz University of Technology (A); 2013.
- [22] Stuefer A. Einflussparameter auf die Querkzugfestigkeit von BSH-Lamellen. Masterarbeit: Graz University of Technology (A); 2011.
- [23] Dill-Langer G. Schädigung von Brettschichtholz bei Zugbeanspruchung rechtwinklig zur Faserrichtung. Dissertation, Materialprüfungsanstalt Universität Stuttgart (D); 2004.
- [24] Riberholt H, Enquist B, Gustafsson PJ, Jensen RB. Timber beams notched at the support. No 280 Serie R, Department of Structural Engineering, Technical University of Denmark; 1992.
- [25] Mau TJ. Time and size effects for tension perpendicular to grain in wood. Thesis. University of British Columbia (USA); 1976.
- [26] Barret JD. Effect of size on tension perpendicular-to-grain strength of Douglas-fir. *Wood Fiber* 1974;6(2):126–43.
- [27] Neuhaus FH. Elastizitätszahlen von Fichtenholz in Abhängigkeit der Holzfeuchtigkeit. Dissertation. Ruhr Universität, Bochum (D); 1981.
- [28] Hörig H. Anwendung der Elastizitätstheorie anisotroper Körper auf Messungen an Holz. *Ing-Arch* 1935;6:8–14.
- [29] Kollmann FP, Cote WA. Principles of wood science and technology – solid wood. Berlin (D): Springer Verlag; 1968.
- [30] Carrington H. The elastic constants of spruce. *Phil. Mag. S. 6* 1923;45(269).
- [31] Stamer J. Elastizitätsuntersuchungen an Hölzern. *Ingenieur-Archiv* 1935;6:1–8.
- [32] Görlacher R. Ein Verfahren zur Ermittlung des Rollschubmoduls von Holz. *Holz Roh Werkst* 2002;60:317–22.
- [33] Fellmoser P, Blaß HJ. Influence of rolling shear modulus of strength and stiffness of structural bonded timber elements. *Proceeding of 37th CIB-W18-meeting*, Edinburgh (UK); 2004.
- [34] EN 408:2010 Timber structures – structural timber and glued laminated timber – determination of some physical and mechanical properties. CEN.
- [35] Mestek P. Punktgestützte Flächentragwerke aus Brettspertholz (BSP) – Schubmessung unter Berücksichtigung von Schubverstärkungen. Doctoral Thesis. Technical University of Munich (D); 2011.
- [36] Blaß HJ, Flaig M. Stabförmige Bauteile aus Brettspertholz. *Karlsruher Berichte zum Ingenieurholzbau 24*. Universitätsverlag Karlsruhe (D); 2012.
- [37] Ehrhart T. Materialbezogene Einflussparameter auf die Rollschubbeigenschaften in Hinblick auf Brettspertholz. Masterarbeit: Graz University of Technology (A); 2014.
- [38] Ehrhart T, Brandner R. Rolling shear: test configurations and properties of some European soft- and hardwood species. *Eng Struct* 2018;172:554–72.
- [39] Wallner G. Versuchstechnische Ermittlung der Verschiebungskenngrößen von orthogonal verklebten Brettlamellen. Diplomarbeit, Graz University of Technology (A); 2004.
- [40] Franzoni L, Lebee A, Lyon F, Foret G. Bending behaviour of regularly spaced CLT panels. *Proceeding of WCTE*, Vienna (A); 2016.
- [41] Jakobs A. Zur Berechnung von Brettlagenholz mit starrem und nachgiebigem Verbund unter plattenartiger Belastung mit besonderer Berücksichtigung des Rollschubes und der Drillweichheit. Dissertation, Bundeswehr University Munich (D); 2005.
- [42] Aicher S, Dill-Langer G. Basic considerations to rolling shear modulus in wooden boards. *Otto-Graf-J* 2000;11.
- [43] Bendtsen BA. Rolling shear characteristics of nine structural softwoods. *For Prod J* 1976;26(11):51–6.
- [44] Hirschmann B. Ein Beitrag zur Bestimmung der Scheibenschubfestigkeit von Brettspertholz. Masterarbeit: Graz University of Technology (A); 2011.
- [45] Brandner R, Bogensperger T, Schickhofer G. In plane shear strength of cross laminated timber (CLT): test configuration, qualification and influencing parameters. *Proceeding of 46th CIB-W18-meeting*, Vancouver (Canada); 2013.
- [46] Spengler R. Festigkeitsverhalten von Brettschichtholz unter zweiachsiger Beanspruchung. *Berichte zur Zuverlässigkeitstheorie der Bauwerke*, Heft 62/1982, Technical. University of Munich (D); 1982.
- [47] Müller U, Sretenovic A, Gindl W, Grabner M, Wimmer R, Teischinger A. Effect of macro- and micro-structural variability on the shear behaviour of softwood. *IAWA J* 2004;25(2):231–43.
- [48] Schäfers M. Entwicklung von hybriden Bauteilen aus Holz und hochfesten bzw. ultrahochfesten Betonen. Dissertation, University of Kassel (D); 2010.
- [49] Brandner R, Gatterner W, Schickhofer G. Determination of shear strength of structural and glued laminated timber. *Proceeding of 45th CIB-W18-meeting*, Växjö (S); 2012.
- [50] Blaß HJ. Ermittlung des 5%-Quantils des Produktes aus Elastizitätsmodul und Torsionsschubmodul für BSH. *Forschungsbericht der Versuchsanstalt für Stahl, Holz und Steine der Universität Karlsruhe (D)*; 2006.
- [51] Brandner R, Gehri E, Bogensperger T, Schickhofer G. Determination of modulus of shear and elasticity of GLT and related examinations. *Proceeding of 40th CIB-W18-meeting*, Bled (SLO); 2007.
- [52] Brandner R, Freytag B, Schickhofer G. Determination of shear modulus by means of standardized four-point-bending tests. *Proceeding of 41th CIB-W18-meeting*, St. Andrews (Canada); 2008.
- [53] Görlacher R, Kürth J. Determination of shear modulus. *Proceeding of 27th CIB-W18-meeting*, Sidney (Australia); 1994.
- [54] Ehlbeck J, Siebert W. Praktikable Einleimmethoden und Wirkungsweise von Gewindestangen unter Axialbelastung bei Übertragung von großen Kräften und bei Aufnahme von Querkugkräften in Biegeträgern. Teil 1: Einleimmethoden, Meßverfahren, Haftspannungsverlauf. Bericht, Versuchsanstalt für Stahl, Holz und Steine, University of Karlsruhe (D); 1987.
- [55] Ringhofer A, Schickhofer G. Investigations concerning the force distribution along axially loaded self-tapping screws. *Materials and joints in timber structures*, RILEM Bookseries 2014;9:201–10.
- [56] Brandner R, Ringhofer A, Grabner M. Probabilistic models for the withdrawal behaviour of single self-tapping screws in the narrow face of cross laminated timber (CLT). *Eur J Wood Prod* 2018;76:13–30.
- [57] Madsen B, Hooley RF, Hall CP. A design method for bearing stresses in wood. *Can J Civil Eng* 1982;9:338–49.
- [58] Tanahashi H, Okamura M, Suzuki Y. Simple formulation of elasto-plastic embedment behaviour of orthotropic wood considering densification. *Proceeding of the WCTE*. Japan: Miyazaki; 2008.
- [59] Tanahashi H, Shimizu H, Suzuki Y. Elastic surface displacements of orthotropic wood due to partial compression based on Pasternak model. *J Struct Constr Engl* 2006(609):129–36.
- [60] Barber JR. Intermediate mechanics of materials. *Solid mechanics and its applications* 175, 2nd ed.; 2000.
- [61] Ehlbeck J, Görlacher R, Werner H. Determination of perpendicular-to-grain tensile stresses in joints with dowel-type fasteners. *Proceeding of 22th CIB-W18-meeting*, Berlin (D); 1989.
- [62] Van der Put TACM. Derivation of the bearing strength perpendicular to the grain of locally loaded timber blocks. *Holz Roh Werkst* 2008;66:409–17.
- [63] Leijten AJM, Jorisson AJM, de Leijer BJC. The local bearing capacity perpendicular to grain of structural timber elements. *Constr Build Mater* 2012;27:54–9.
- [64] Brandner R. Cross laminated timber (CLT) in compression perpendicular to plane: testing, properties, design and recommendations for harmonizing design provisions for structural timber products. *Eng Struct* 2018;171:944–60.
- [65] EN 1382:1999 Timber structures – test methods – withdrawal capacity of timber fasteners. CEN.
- [66] EN 26891:1991 Timber structures – joints made with mechanical fasteners – general principles for the determination of strength and deformation characteristics. CEN.
- [67] Zhou X-H, Gao S. Confidence intervals for the log-normal mean. *Stat Med* 1997;16:783–90.
- [68] Olsson U. Confidence intervals for the mean of a log-normal distribution. *J. JSE* 2005;13(1).
- [69] Blaß HJ, Uibel T. Tragfähigkeit von stiftförmigen Verbindungsmitteln in Brettspertholz. *Forschungsbericht: University of Karlsruhe (D)*; 2007.
- [70] Plüss Y, Brandner R. Untersuchungen zum Tragverhalten von axial beanspruchten Schraubengruppen in Brettspertholz (BSP). 20. Internationales Holzbau-Forum, Garmisch-Partenkirchen (D); 2014.
- [71] Ringhofer A, Brandner R, Schickhofer G. A universal approach for withdrawal properties of self-tapping screws in solid timber and laminated timber products. *Proceeding of 2nd INTER-meeting*, Sibenik (Croatia); 2015.